Received: 13 January 2021 | Accepted: 22 February 2021

DOI: 10.1002/gea.21858

RESEARCH ARTICLE

Geoarchaeology An International Journal WILEY

Multianalytical investigation of wasters from the Tower 8/Porta di Nola refuse middens in Pompeii: Sr–Nd isotopic, chemical, petrographic, and mineralogical analyses

Vincenza Guarino[1] | Alberto De Bonis[1,2] | J. Theodore Peña[3] | Maria Verde[1] | Vincenzo Morra[1,2]

[1]Dipartimento di Scienze della Terra, dell'Ambiente e delle Risorse (DiSTAR), Università degli Studi di Napoli Federico II, Napoli, Italy

[2]CRACS, Center for Research on Archaeometry and Conservation Science, Napoli, Italy

[3]Department of Classics, University of California–Berkeley, Berkeley, California, USA

Correspondence
Vincenza Guarino and Alberto De Bonis, Dipartimento di Scienze della Terra, dell'Ambiente e delle Risorse (DiSTAR), Università degli Studi di Napoli Federico II, Napoli, Italy.
Email: vincenza.guarino@unina.it and alberto.debonis@unina.it

Funding information
Dipartimento di Scienze della Terra, dell'Ambiente e delle Risorse (Vincenzo Morra) of the Università degli Studi di Napoli Federico II

Abstract

A total of nine representative pottery fragments belonging to ferruginous, carbonate, and thin-walled wares were recovered in refuse middens outside the fortification wall of Pompeii and subjected to a program of multianalytical operations (thermal ionization mass spectrometry, X-ray fluorescence, X-ray powder diffraction analysis, scanning electron microscopy–energy-dispersive spectrometry techniques, optical microscopy). The fragments bear manufacturing defects, indicating their local production in workshops located somewhere at Pompeii. These three groups display a similar volcanic coarse component that exhibits distinct chemical compositions. The volcanic component consists of alkali feldspar, clinopyroxene, plagioclase, minor garnet, and rock fragments (with primarily plagioclase and leucite), pointing to an origin from the Somma-Vesuvius. The fingerprint of the Sr–Nd isotopes of carbonate ware suggests an affinity with high-CaO clays from Rufoli, a subdivision of Salerno. Sr–Nd isotopes also suggest that clays from the Sorrentine Peninsula were used: A clay mixture of different argillified pyroclastic materials was employed for the low-CaO ferruginous ware, whereas the low-CaO thin-walled ware was manufactured with a marine varicolored clay. The distribution of materials likely occurred by sea via the port at Salernum and Surrentum. The combination of different types of complementary data obtained through this program of analysis illustrates the importance of combining both quantitative petrographic and chemical characterization in the evaluation of archaeological pottery.

KEYWORDS

carbonate ware, clay, ferruginous ware, multianalytical analysis, Pompeii, pottery production, Sr–Nd isotopes, thin-walled ware

Scientific editing by Ian Moffat.

1 | INTRODUCTION

A variety of research projects carried out at the ancient Roman town of Pompeii in recent years has substantially enlarged the body of evidence at our disposal regarding the local manufacture of pottery (Cavassa, 2009; Cavassa et al., 2013, 2015; Ellis et al., 2015; Grifa et al., 2021a; Peña & McCallum, 2009a, 2009b; Toniolo & Osanna, 2020). This evidence includes the remains of pottery workshops that contain production fixtures (clay mixing basins, mounting pits for potter's wheels, kilns), potter's tools, and unused raw materials, as well as vessels and vessel fragments recovered either at these establishments or at other locales in or near the town that exhibit manufacturing defects, indicating that they are wasters discarded in the course of the manufacturing process. This evidence has the potential to provide new insights into the different wares and forms manufactured at Pompeii, as well as the geography, organization, technology, and chronology of Pompeiian pottery production. To date, there has been little research directed toward the technological and compositional characterization of the pottery bearing manufacturing defects that have been recovered at these workshops and elsewhere at Pompeii, and our understanding of pottery manufacture in the town remains substantially underdeveloped. This stands in distinct contrast to our knowledge of several other kinds of craft activities at Pompeii and of the economic life of the town, more generally.

This study reports the results of a multianalytical investigation (thermal ionization mass spectrometry [TIMS], X-ray fluorescence [XRF], X-ray powder diffraction analysis [XRPD], scanning electron microscopy–energy-dispersive spectrometry [SEM-EDS] techniques, optical microscopy [OM]) involving a representative set of fragments of waster pottery recovered in deposits of mixed refuse dumped immediately outside the town's fortification walls. These fragments likely originated at an as-yet-undiscovered pottery workshop located somewhere in the unexcavated part of the town.

The program of analysis was aimed at determining the following:

- the general nature of the raw materials employed for the manufacture of the vessels;
- the likely locations of the sources of these raw materials; and
- the paste preparation and firing practices employed in the manufacturing process.

More generally, the determination of the specific compositional characteristics of pottery manufactured at Pompeii will facilitate the recognition of pottery of Pompeiian origin recovered both at Pompeii and at other archaeological sites.

2 | THE ARCHAEOLOGICAL CONTEXT AND THE POTTERY ANALYZED

In 1978, an archaeological team from the Università Statale di Milano under the direction of C. Chiaramonte Trerè excavated a set of three large refuse deposits consisting of mixed material that had been dumped against the outer face of Pompeii's fortification wall in the north–central part of its circuit, between Tower 8 to the west and the Porta di Nola (Nola Gate) to the east (Chiaramonte Trerè, 1986) (Figure 1a,b). The Milan team subsequently published a catalog of the pottery, ceramic lamps, and vessel glass recovered in these features (Romanazzi & Volontè, 1986). During the years 2014–2016, a team from the University of California, Berkeley, under the direction of one of the authors (J. T. P.) undertook a comprehensive evaluation of the full set of materials recovered in these four deposits as part of the Pompeii Artifact Life History Project (PALHIP), a long-term research program aimed at elucidating various aspects of artifact life history at Pompeii through the detailed evaluation of selected sets of artifacts recovered in the course of various excavations at Pompeii or sites in its environs (Peña, 2020). In the course of this study, the PALHIP team recognized a modest number of pottery fragments that bore more or less prominent manufacturing defects (vessels marked by distortion and/or cracking, with ceramic bodies that display conspicuous reduction or discoloration, advanced vitrification, and/or bloating), and on the basis of this evidence, it inferred that these deposits had received small amounts of refuse originating at a pottery workshop (or, less probably, two or more workshops) likely located somewhere in the unexcavated part of the town, presumably at no great distance from this segment of the fortification wall. The available evidence indicates that this workshop was active for some undefinable period of time during the final quarter of the first-century BCE and/or the first half of the first-century CE. The PALHIP team evaluated the ceramic body of the fragments of waster pottery and fragments of pottery from these deposits that did not bear obvious manufacturing defects that were judged likely to be products of the same workshop. A macroscopic description of the fabrics, basically very close to the indications proposed by Orton and Hughes (2013) and in Fabrics of the Central Mediterranean (FACEM) (http://facem.at/project/about.php#method), was made by examining an untreated fracture surface under low magnification (ca. ×10–70) using a Dino-Lite AM 413T digital microscope (see Supporting Information Material).

On the basis of this evaluation, we recognized three distinct groups of pottery:

Group 1: bottles, jars, lids, planting pots, and possibly other forms with a coarse reddish ceramic body containing abundant, small to medium inclusions of volcanic origin.

Group 2: jars, bowls, and basins, and possibly other forms with a light-colored ceramic body containing sparse to frequent, small to medium inclusions of volcanic origin.

Group 3: thin-walled beakers and bowls in a gritty, reddish ceramic body containing abundant small inclusions of volcanic origin.

On the basis of our geological knowledge of regional clay resources and the exploitation of these by both ancient potters and traditional potters in historically recent times (Peña & Kane, 2016), the PALHIP team conjectured that the preparation of the pastes from which the vessels in these three groups were manufactured involved the following (Table 1):

Group 1: the use of an unmodified (or largely unmodified?) "ferruginous" clay derived from the argillification of a parent material of volcanic origin;

Group 2: the addition of volcanic sand temper to a carbonate clay of probable marine origin;

Group 3: the use of a "ferruginous" clay derived from the argillification of a parent material of volcanic origin, possibly a fine fraction of the clay employed for the manufacture of Group 1.

The PALHIP team and the archaeometric research group based in the Dipartimento di Scienze della Terra, dell'Ambiente e delle Risorse, University of Naples Federico II, subsequently initiated a collaborative program of analysis involving these materials. This represents an extension of the Naples group's ongoing program of research involving the mineralogical and chemical characterization of archaeological pottery and relevant geologic materials from the broader Campania region. The *Parco Archeologico di Pompei* approved a program of analysis that involved the characterization of a limited number of specimens, reflecting the fact that the application of the suite of analytical procedures proposed envisaged the destruction of a small, though not insignificant amount (ca. 1–2 g) of each specimen analyzed. The PALHIP team accordingly selected a set of specimens for analysis that included three examples of each of the three groups that it had identified—designating these as PomT8PN1–9—with the assumption that this might permit—if only in a very minimal way—the recognition of a general group composition for

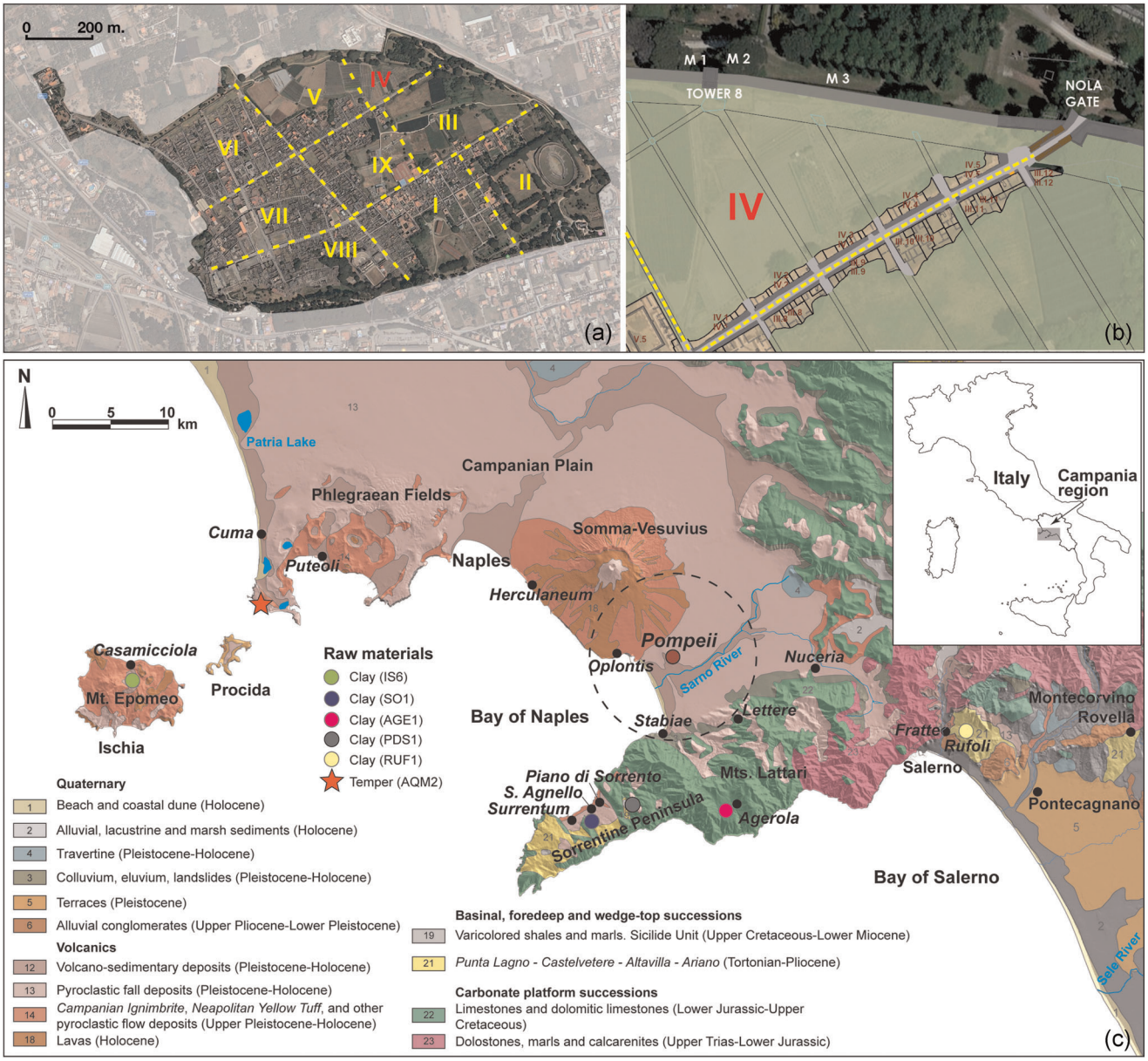

FIGURE 1 (a) Generalized archeological area of Pompeii and its relative sectors (modified after https://www.visitpompeiivesuvius.com/it/pompei). (b) Composite satellite image/map showing area of Pompeii Tower 8/Nola Gate excavations (sector IV); M, midden. (Courtesy: Eric Poehler/Pompeii Bibliography and Mapping Project; modified after Peña, 2020). (c) Generalized geologic map of the greater Bay of Naples region (GBNR) marked with a circle with a radius of 7 km centered on Pompeii (modified after De Bonis et al., 2018) [Color figure can be viewed at wileyonlinelibrary.com]

TABLE 1 Sampling data

Samples ID	Pottery group/material type	PALHIP group	PALHIP ID	Vessel form/part	Manufacturing defects	Analytical techniques
PomT8PN2	Ferruginous ware (FW)	Group 1	PALHIP0206	Planting pot base	No manufacturing defects	VI, OM, XRPD, XRF
PomT8PN3			PALHIP0207	Planting pot base	Reduced, vitrified	VI, OM, XRPD, XRF, EDS, SEM, TIMS
PomT8PN4			PALHIP0208	Lid knob	Reduced, vitrified?, deformed	VI, OM, XRPD, XRF, TIMS
PomT8PN1	Carbonate ware (CW)	Group 2	PALHIP0203	Jar base	Greenish color, vitrified surface	VI, OM, XRPD, XRF
PomT8PN7			PALHIP3067	Jar rim/handle	Greenish color	VI, OM, XRPD, XRF, EDS, SEM, TIMS
PomT8PN8			PALHIP0368	Jar rim/handle	Greenish color	VI, OM, XRPD, XRF
PomT8PN5	Thin-walled ware (TWW)	Group 3	PALHIP0210	Beaker base	Reduced surface, cracked	VI, OM, XRPD, XRF, EDS, SEM, TIMS
PomT8PN6			PALHIP0278	Beaker rim	Reduced surface	VI, OM, XRPD, XRF
PomT8PN9			PALHIP0528	Beaker base	Reduced, vitrified, deformed	VI, OM, XRPD, XRF

Samples ID	Pottery group/ material type	Site (code of Italian Province)	Origin	Geological information	Analytical techniques
SO1[a]	Clayey raw material	Sant'Agnello (NA)	LCC volcanic	Weathered pyroclastics from eruptions of Neapolitan volcanoes younger than the Campanian Ignimbrite (39 ky)	XRF[a], TIMS[d]
AGE1	Clayey raw material	Agerola (NA)	LCC volcanic	Weathered pyroclastics from eruptions of Neapolitan volcanoes younger than the Campanian Ignimbrite (39 ky)	XRF, TIMS
RUF1[a]	Clayey raw material	Rufoli di Ogliara (SA)	HCC marine	Altavilla Group wedge-top basin deposit (upper Messinian–lowermost Pliocene)	XRF[a], TIMS
PDS1	Clayey raw material	Piano di Sorrento (NA)	LCC marine	Varicolored clays olistostromes in Castelvetere wedge-top deposit (upper Tortonian–lower Messinian)	XRF, TIMS
IS6[a]	Clayey raw material	Ischia (NA)	HCC marine	Cava Leccie unit (upper Pleistocene)	XRF[a], TIMS[d]
AQM/AQM2[b,c]	Local volcanic sand	Monte di Procida (NA)			XRF[b,c], TIMS[d]

Note: Data from (a) De Bonis et al. (2013); (b) Morra et al. (2013); (c) De Bonis et al. (2014); (d) De Bonis et al. (2018).

Abbreviations: HCC, high-CaO clay; LCC, low-CaO clay; NA, Naples; OM, optical microscopy; PALHIP, Pompeii Artifact Life History Project; SA, Salerno; SEM-EDS, scanning electron microscopy–energy-dispersive spectrometry; TIMS, thermal ionization mass spectrometry; VI, visual inspection; XRF, X-ray fluorescence; XRPD, X-ray powder diffraction.

each of the three groups and perhaps also the identification of any compositional outliers. For all three groups, the three specimens selected were rim or base/knob fragments that clearly belonged to different vessels. For Groups 1 and 3, the set of specimens included a specimen that was unambiguously a waster, a second specimen that was thought likely to be a waster, and a third specimen that, while highly similar to one of the first two specimens in form, dimensions, and technique, and thought perhaps to belong to the same kiln load in which that other specimen had been fired, had a ceramic body that displayed more regular firing (rather than advanced vitrification and reduction), as this facilitated the characterization of the ceramic body and was thought likely to permit the acquisition of more complete and indicative information regarding texture, mineralogical composition, and firing temperature. The set of materials displaying manufacturing defects that was available for Group 2 was somewhat more limited than it was for the other two groups, and the three specimens selected were all specimens that were judged to be a probable or possible waster that did not display either advanced vitrification or reduction.

The three pottery groups, their manufacturing defects, and related profile, identified by the PALHIP team, were referred here as follows (Table 1, Figure 2, and Supporting Information Material):

- PALHIP Group 1: ferruginous ware (FW);
- PALHIP Group 2: carbonate ware (CW);
- PALHIP Group 3: thin-walled ware (TWW).

3 | RAW MATERIALS FOR POTTERY PRODUCTION AT POMPEII

Clayey raw materials in the Campania region are mainly located in the Apennine basinal and, to a lesser extent, alluvial sediments. Minor deposits also originated from intensive weathering of pyroclastic products associated with the eruptions of Campanian volcanoes (Somma-Vesuvius, Phlegraean Fields, Roccamonfina). In the Bay of Naples area, which includes Pompeii and other important productive centers of pottery, the presence of accessible raw materials is more limited (De Bonis et al., 2013).

From a geological point of view, the greater Bay of Naples region (GBNR) is dominated by the presence of two important volcanic centers, the Somma-Vesuvius Volcanic Complex (SVVC) and the Phlegraean Fields, which include both continental and insular sectors. Both volcanoes constitute the Campanian Volcanic District (CVD), which forms the southern part of the Roman Magmatic Province (e.g., Avanzinelli et al., 2009; Conticelli et al., 2004; Morra et al., 2010). The two volcanic areas are characterized by volcanic products displaying a potassium shoshonitic series in the case of both the Phlegraean Fields and the SVVC and a high-potassium leucite-bearing series in the case of the SVVC. These two volcanic areas, which have strongly conditioned life in this part of the region of Campania throughout history, are typically characterized by explosive eruptions, followed by periods of quiescence. Pompeii is located within the SVVC on the southern flank of the Somma-Vesuvius stratovolcano, 9 km to the southeast of the current vent of Mount Vesuvius and 20 km to the southeast of the modern city of Naples (Figure 1c).

To identify the raw materials used for the production of pottery at Pompeii, we focused our attention on the outcrops closest to the city and those that, despite being located at some distance, are more widespread and, in some cases, have been employed in historically recent times for the traditional production of ceramics.

Ethnographic studies of traditional potters indicate that in the vast majority of cases, these craftsmen employ clay and tempering material obtained from sources located within no more than ca. 7 km of the locus of manufacture (Arnold, 2006; Kelly et al., 2011). This practice is substantially a function of the wide availability of potting

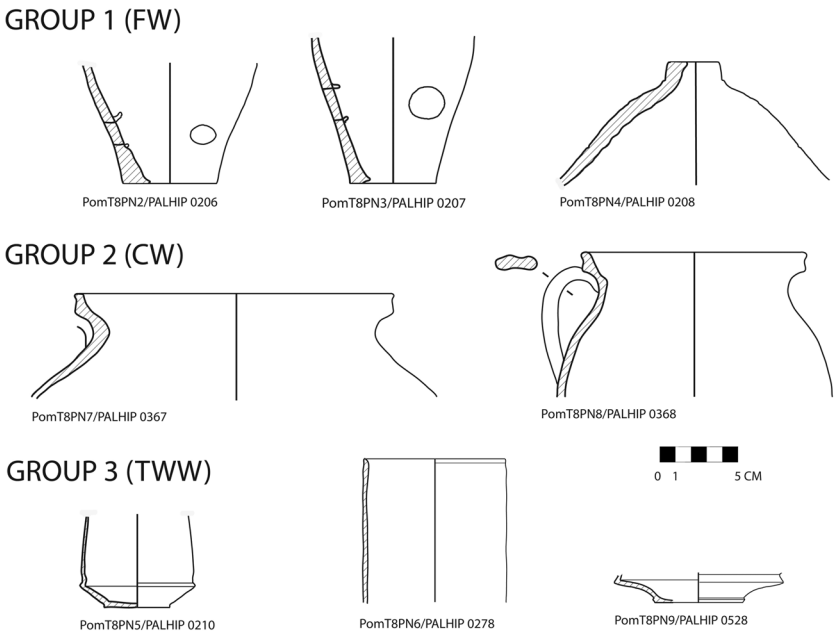

FIGURE 2 Profile drawings for eight of nine specimens analyzed. (No drawings are available for PomT8PN1/PALHIP0203). CW, carbonate ware; FW, ferruginous ware; TWW, thin-walled ware

clays and tempering materials in most regions, combined with the costs of time and effort involved in traveling to a raw material source and in transporting the material acquired to the workshop location. Given the absence of the means for efficient, low-cost land transport in the Roman world, it seems likely that a generally similar dynamic was in operation there, and to formulate a first approximation of the set of raw materials that would have been preferred for use by Pompeiian potters, we can attempt to identify the set of clays and tempering materials suitable for pottery manufacture that would have been available within 7 km of the town. To facilitate such an undertaking, Figure 1c presents a generalized geologic map of the GBNR marked with a circle with a radius of 7 km centered on Pompeii. Over nearly the whole of the territory defined by this circle, the terminal portion of the geologic sequence consists of formations belonging to the SVVC. The northwest, ca. one-third of this territory consists of SVVC lavas and pyroclastic deposits that make up the southern flank of the Vesuvius stratovolcano, whereas nearly the whole of the remainder consists of SVVC pyroclastic deposits that blanket the northern and southern flanks of the middle/lower Sarno River Valley. The floodplain of the Sarno River traverses the territory in a narrow band running from northeast to southwest, passing immediately to the south of Pompeii before reaching the coast a short distance to the southwest of the town. In this area, the floodplain is composed of sediments that consist of volcanic materials derived from the SVVC and sedimentary materials that contain calcite due to the contribution of material derived from the limestone formations that make up the east–west chain of the Monti Lattari (Morra et al., 2013), which forms the southern boundary of the Sarno floodplain.

Geomorphological changes that occurred as a result of the 79 CE eruption of Mount Vesuvius (and, to a more limited extent, its subsequent eruptions) (Albore Livadie et al., 1990; Seiler et al., 2011) that buried much of the area around Pompeii with volcanic ejecta, along with heavy anthropization and urban development, have rendered the locating of ancient raw material sources by modern researchers extremely difficult in this territory. Despite these changes, the pattern of geologic formations described is similar in general terms to the one that would have characterized this area during the centuries preceding this event.

The relevant geologic map (Istituto Superiore per la Protezione e la Ricerca Ambientale, ISPRA, 2015, f. 466–485) and explanatory notes indicate only a very limited presence of argillaceous deposits within this territory, and the authors are not aware of any clay outcrop in this area that was exploited for ceramic production in historically recent times. On the basis of the geologic situation, it seems likely that during the centuries preceding the 79 CE eruption of Mount Vesuvius, the territory contained only a limited set of clay deposits of potentially two different kinds that could have been exploited for the manufacture of pottery.

With regard to the first of these, it can be conjectured that in some locations there were occurrences of SVVC pyroclastic deposits that had been subjected to extensive weathering, resulting in the formation of clay minerals. Argillified pyroclastic deposits of this kind are a common occurrence on hillslopes in the volcanic landscapes of Campania and occur either as in situ deposits or as colluvium and landslide deposits (De Bonis et al., 2013). In historically recent times, materials of this kind have been employed for the manufacture of pottery—cookwares, in particular—at some locations in the Roman Magmatic Province, for example, Vasanello [Province of Viterbo] (Peña, 1992) and northern Campania region, Cascano [Province of Caserta] (De Bonis et al., 2013; Peña, 1992), and this may well have been the case during the Roman period. The second kind of clay deposit that we can conjecture for this territory would take the form of Sarno sediments consisting of pelites belonging to the Agro nocerino-sarnese subsynthem (ISPRA, 2015, f. 466–485), associated with volcanoclastic silty sands of fluvial/marsh environment, often containing organic matter or peat (A. Cinque, 1991). Although it would have been desirable to include in this analysis clay specimens obtained from deposits of argillaceous sediment on the Sarno floodplain in the environs of Pompeii, this was not possible, as these are inaccessible for sampling due to the presence of several meters of pyroclastic overburden (Vogel et al., 2011).

Deposits of material suitable for use as a temper, in contrast, would have been widely available in the environs of Pompeii in the form of volcanic sand that had weathered out of SVVC formations. These rocks vary from potassic to ultrapotassic (e.g., Conticelli et al., 2004), with the degree of alkalinity and thus silica undersaturation increasing with time from (1) weakly silica-undersaturated (potassic series or KS) pre-caldera products (>8.9 ka), through (2) mildly silica-undersaturated (high-potassic series or HKS) syn-caldera products (from 8.9 ka to 79 CE), eventually to (3) strongly silica-undersaturated (HKS) post-caldera products (younger than the 79 CE eruption). KS rocks range in composition from K-trachybasalts to trachytes. Rocks of the mildly undersaturated HKS are phonotephrites, tephriphonolites, and phonolites, whereas those belonging to the highly undersaturated HKS range from leucite tephrite to leucite phonolite. The sands derived from these formations accordingly consist of grains of leucite, clinopyroxene, alkali feldspar, plagioclase, biotite, and olivine, with accessory garnet (Joron et al., 1987), along with volcanic lithics and leucite-bearing scoriae. Although volcanic sand of this kind would have been present in some larger or smaller amount in virtually any depositional basin, either at or in the environs of Pompeii, it probably would have proved convenient for Pompeii potters to obtain tempering material in quantity by collecting beach sand at some location along the shore somewhere in the immediate vicinity of the town. To the north of the mouth of the Sarno River, deposits of beach sand are composed almost exclusively of volcanic material derived from SVVC formations, whereas at the mouth of the river and along the coast to the south, these consist of a mixture of material originating in SVVC formations and carbonate rock fragments derived from the Monti Lattari (Garzanti et al., 2002; Morra et al., 2013).

It is widely accepted by scholars of the Roman world that the transport of cargoe by water would have been substantially less costly than their transport overland (e.g., Greene, 1986). The fact that Pompeii was situated on the coast and functioned as a port, thus, raises the prospect that the potters who worked there obtained their raw materials from sources located beyond the immediate environs of the town, especially in cases in which a source was

situated on or near the coast and would have enjoyed convenient access to a port. We can, in fact, conjecture that the limited availability of deposits of clay suitable for the manufacture of pottery in the immediate environs of the town might have encouraged or, even to some extent, obliged potters working at Pompeii to employ clay obtained from more distant sources.

Five clay sources are worthy of consideration in this regard. The first of these is an ill-defined and apparently dispersed set of argillified pyroclastic deposits located in the area of Sant'Agnello on the north shore of the Sorrentine Peninsula, ca. 13–15 km to the southwest of Pompeii (Figure 1c). In historically recent times, brick and tile makers active at Maiano, a subdivision of Sant'Agnello, have employed this raw material to manufacture brick and tiles, with a particular focus on tiles with exceptional heating and heat retention properties that are widely employed in the GBNR and beyond to line pizza ovens (De Bonis et al., 2013, 2014; Peña & Kane, 2016). In recent years, these craftsmen have obtained this material adventitiously, collecting it as spoil at construction sites at various locations within the municipalities of Sant'Agnello and Piano di Sorrento, immediately to its east. The parent formation for this material is reported on the geologic map for this area (ISPRA, 2015, f. 466–485, VEF_1) as consisting of reworked weathered pyroclastics belonging to the Vesuvian–Phlegraean synthem younger than the Campanian Ignimbrite (39 ky). De Bonis et al. (2014) have analyzed a sample of this material, showing that it is characterized geochemically by a low concentration of CaO and contains frequent coarse mineral grains and rock fragments typical of the SVVC with an admixture of fine to coarse sedimentary material derived from adjacent formations, including quartz, sandstone, and carbonate rock. The sources of this material are situated within no more than 2.5 km of the coast and would have lain no more than ca. 3 km from the harbor at Roman Surrentum, meaning that this material, which would have been suited for the manufacture of heavy utilitarian vessels, could have been distributed by sea to distant coastal locations at moderate cost.

In the whole Sorrentine Peninsula, variously extended argillified pyroclastic deposits are present locally. With regard to these, we have evidence of a clayey level located in the plain of Agerola (Figure 1c), as the second clay source, represented by weathered pyroclastics from eruptions of Neapolitan volcanoes younger than the Campanian Ignimbrite (39 ky). The fact that ruins of ancient furnaces were found in Agerola, immediately below the pumices of A.D. 79, strongly suggests the presence of craft activity in Roman times in the area (M. Cinque, 2015).

The third of these sources is a deposit of a high-CaO marine clay ascribed to Apennine wedge-top basin successions of the Altavilla Group (upper Messinian–lowermost Pliocene; Vitale & Ciarcia, 2018) that outcrops over an extensive area at Rufoli di Ogliara, a subdivision of Salerno, ca. 28 km to the east–southeast of Pompeii (De Bonis et al., 2013; Peña & Kane, 2016; Scarpelli et al., 2017). In historically recent times, this clay has been employed by workshops located at Rufoli di Ogliara for the manufacture of architectural ceramics and has been distributed to various locations across southern Italy for the manufacture of pottery. This outcrop lies ca. 4 km from the coast and would have lain ca. 5 km from the harbor at Roman Salernum, meaning that in Roman times, this material, which would have been suited for the manufacture of tablewares, lamps, and utilitarian vessels, could have been distributed by sea to distant coastal locations at moderate cost. There is an extensive outcrop of the same formation at Montecorvino Rovella (De Bonis et al., 2013), 18 km to the east of Salerno and 39 km to the east–southeast of Pompeii, that has been employed in historically recent times by workshops operating in that town for the manufacture of architectural ceramics and pottery (Peña & Kane, 2016). To the authors' best knowledge, the Rufoli di Ogliara outcrop is the source of marine clay closest to Pompeii that would have been extensive enough to support ceramic production in the town at an appreciable scale over a prolonged period of time. Scarpelli et al. (2014, 2017) analyzed a set of black-gloss ware vessels from Pompeii and clay specimens from both Rufoli di Ogliara and Montecorvino Rovella, concluding that these vessels might have been manufactured with clay from either of these two sources. More recently, a multianalytic program of archaeometric analysis involving a pottery workshop in the *Via dei Sepolcri*, immediately outside Pompeii's Porta Ercolano (Herculaneum Gate) that specialized in the manufacture of TWW (distinct from the TWW being analyzed in the program of analysis being reported here) (Cavassa et al., 2013, 2015), provided new and remarkable insights into the ceramic production cycle in the town. The outcomes of this study indicate that this production involved the use of marine clay with a composition strikingly similar to that of the clay from the Rufoli di Ogliara and Montecorvino Rovella sources (Grifa et al., 2021a, 2021b).

Worth noting in this connection is that small deposits of marine clay closer to Pompeii than those from Rufoli di Ogliara and Montecorvino Rovella exist at several locations in the Sorrentine Peninsula. We can consider these sediments as the fourth clay source. They occur in the form of olistoliths and olistostromes containing beds of varicolored clays that belong to Castelvetere wedge-top arenaceous deposits (upper Tortonian–lower Messinian; Vitale & Ciarcia, 2018), which in the Sorrentine Peninsula are expressed locally also as “disturbed” clay-rich deposits that occur in reworked and weathered zones affected by landslide activity (Cesarano et al., 2018).

The fifth and last of the nonlocal clay sources worth considering is an extensive set of deposits of moderately calcareous marine clay containing substantial amounts of volcanic mineral grains and rock fragments that belong to the Phlegraean Fields that occur on the north slope of Monte Epomeo on the Island of Ischia, ca. 50 km to the west of Pompeii (Cava di Leccie unit; upper Pleistocene; Barra et al., 1992; De Bonis et al., 2013, 2014). In historically recent times, clay from these deposits was employed by potters at Casamicciola, a town on the north shore of Ischia, for the manufacture of architectural ceramics and pottery (Olcese, 2011). Documentary evidence indicates that this clay was transported to Naples for the manufacture of ceramics during the 18th and 19th centuries (Buchner, 1994), and compositional studies suggest that it was also transported there and to other locales in the GBNR during the Greek and Roman periods for the manufacture of

pottery (e.g., De Bonis et al., 2016; Greco et al., 2014; Grifa et al., 2009, 2016, 2019; Munzi et al., 2014). The sources of this material, which would have been suited for the manufacture of tablewares and storage vessels, are situated no more than ca. 2 km from the coast and would have lain within no more than ca. 3–5 km of the Roman port at Aenaria, meaning that in Roman times, it could have been distributed by sea to distant coastal locations at a moderate cost.

These five raw materials are listed in Table 1, which include, in the order described above, Sant'Agnello clay (SO1) and Agerola clay (AGE1) as argillified pyroclastic deposits, Rufoli di Ogliara (RUF1) as a high-CaO marine clay ascribed to Apennine wedge-top basin successions of the Altavilla Group, a varicolored clay type from Piano di Sorrento (PDS1), and an Ischia Monte Epomeo North clay specimen (IS6).

4 | ANALYTICAL TECHNIQUES

The nine specimens of pottery, and abovementioned raw materials, were subjected to a battery of analyses selected with a view to elucidate the research questions indicated above. The set of operations to which each of the specimens was subjected is indicated in Table 1.

4.1 | OM

Basic features of the ceramic body, including texture, color, and birefringence of the matrix, and the type, condition, abundance, and sorting of inclusions were evaluated in thin section employing an OPTIKA petrographic microscope equipped with a Zeiss Axiom 105 color camera running ZEN 2.2 (blue edition) software. The abundance, size range, and angularity of inclusions were estimated by reference to comparator charts (Terry & Chilingar, 1955).

4.2 | EDS

The microchemical composition of mineral grains in the ceramic body was determined on polished thin sections at the Dipartimento di Scienze della Terra, dell'Ambiente e delle Risorse (DiSTAR), University of Naples Federico II (JEOL JSM-5310 microscope and Oxford Instruments Microanalysis Unit, equipped with an INCA X-act detector and operating at 15 kV primary beam voltage, 50–100 mA filament current, variable spot size, from ×30,000 to ×200,000 magnification, 20 mm WD and 50 s net acquisition real time). Measurements were made with an INCA X-stream pulse processor and with INCA Energy software. Energy uses the XPP matrix correction scheme, developed by Pouchou and Pichoir (1988), and the pulse pileup correction. The quant optimization is carried out using cobalt (full width at half maximum peak height (FWHM) of the strobed zero = 60–65 eV). The following standards, produced at the Smithsonian Institution, were used for calibration: diopside (Ca), San Carlos olivine (Mg), anorthoclase (Al, Si), albite (Na), rutile (Ti), fayalite (Fe), Cr_2O_3 (Cr, chromite), rhodonite (Mn), orthoclase (K), barite (Ba), celestine (Sr), and pure vanadium (V). All mineral standards are reported in Table S1. The Kα, Lα, and Mα lines were used for calibration, according to the element. Backscattered electron (BSE) images were obtained with the same instrument. Additional details regarding analytical procedures are available in Franciosi et al. (2019) and Guarino et al. (2019). The precision and accuracy of EDS analyses are reported in Rispoli et al. (2019).

4.3 | SEM

A fresh fracture surface of the specimen was examined by SEM to evaluate the degree of sintering undergone by the ceramic body with a view to assist in the estimation of maximum firing temperature (Maniatis & Tite, 1981).

4.4 | XRPD

The bulk mineralogical composition was determined by semiquantitative XRPD using a PANalytical X'Pert PRO 3040/60 PW diffractometer (CuKα radiation, 40 kV, 40 mA; scanning interval, 4–50° 2θ; step size, 0.017° 2θ; counting time 15.5 s/step) (Malvern Panalytical Ltd.).

4.5 | XRF

Bulk chemical composition was determined by means of XRF. Samples were prepared as pressed powder pellets and analyzed using an Axios Panalytical Spectrometer (Malvern Panalytical Ltd.). The samples were assayed for ten major constituents (SiO_2, TiO_2, Al_2O_3, Fe_2O_3, MnO, MgO, CaO, Na_2O, K_2O, P_2O_5), with values expressed as percent weight (wt%), and for twelve trace elements (Rb, Sr, Y, Zr, Nb, Ba, Cr, Ni, Sc, V, La, Ce), with values expressed as parts per million (ppm). Analytical uncertainties were in the order of 1%–2% for the major elements and 5%–10% for trace elements (Cucciniello et al., 2017, 2018). The standards employed are reported in Table S1. Loss on ignition (LOI) was determined by pre-drying 1 g of powdered sample material overnight at 110°C and then heating this to 1000°C.

4.6 | TIMS

The Sr–Nd isotopic composition of representative pottery and clay samples was determined via TIMS. The high compositional homogeneity of the groups allowed us to analyze one sample of CW (PomT8PN7) and TWW (PomT8PN5); from the FW group, two samples were selected (PomT8PN3 and PomT8PN4). Samples PDS1, AGE1, and RUF1 were selected from the clay deposits described in Section 3.

$^{87}Sr/^{86}Sr$ and $^{143}Nd/^{144}Nd$ isotope ratios of PomT8PN7 (CW) and PomT8PN5 (TWW) ceramic samples, and PDS1, AGE1, and RUF1 clays were determined at the Radiogenic Isotope Laboratory of the INGV–OV (Naples, Italy), employing TIMS techniques, to explore the potential that

this method has for determining pottery provenance. The values obtained were normalized in accordance with the recommended values for the NIST SRM 987 ($^{87}Sr/^{86}Sr = 0.71025$) and La Jolla ($^{143}Nd/^{144}Nd = 0.51185$) international standards. Details regarding these analytical procedures are presented in De Bonis et al. (2018). However, $^{87}Sr/^{86}Sr$ and $^{143}Nd/^{144}Nd$ isotope ratios of PomT8PN3 (FW) and PomT8PN4 (FW) ceramic samples were determined at the DiSTAR laboratory (Naples, Italy), using a Thermo Fisher Scientific Triton Plus mass spectrometer equipped with one fixed and eight adjustable Faraday cups. More details are given in Babazadeh et al. (2021). Details regarding the theory of binary mixing (following Langmuir et al., 1978) employed for the interpretation of the data have been described in De Bonis et al. (2018).

4.7 | Principal component analysis (PCA)

PCA was used to reduce the dimensionality of the data set (De Bonis et al., 2016; Hall, 2004; and references therein). Hierarchical clustering analysis (HCA) was applied on the data set reduced by PCA, to cluster samples in a dendrogram using an agglomerative clustering algorithm (Euclidean distance and average linkage method). This operation involved the use of R software (R Development Team) on log10 transformation values of both major and trace element data, omitting some elements (CaO, MnO, P_2O_5, Ba) that are more susceptible to post-burial contamination (Fabbri et al., 1994; Maggetti, 2001). The statistical treatment included data obtained from the analysis of several high-CaO and low-CaO clays from the Campania region to find the best correspondence between the pottery and the type of clay used, considering the geological origin; some of these clays were also subjected to the analysis of the fine fraction obtained by means of a rigorous refining process (data from De Bonis et al., 2013 and other unpublished data). The variance results are given in Table S1, whereas the geologic details of main Campanian clays are presented in Table S2.

5 | RESULTS

5.1 | OM

A representative photomicrograph of the ceramic body of each of the nine specimens is presented in Figures 3–5. The three FW specimens (PomT8PN2, PomT8PN3, PomT8PN4) (Figure 3) exhibit a bimodal distribution of inclusions in an inactive matrix with high porosity. In all three of these specimens, there are abundant, large elongated voids oriented parallel to the vessel's surfaces. The small residual inclusions in the clay matrix consist of quartz and micas (mainly muscovite and subordinate biotite) (Figure 3). Inclusions in the coarse component (~20%–30%) are subangular and include sparse grains of alkali feldspar, Ca clinopyroxene, plagioclase, opaque oxides, amphibole, and garnet (Figure 3), fragments of volcanic rock and scoriae that contain crystals of plagioclase, clinopyroxene, and leucite (Figure 3c,d), and rare argillaceous rock fragments (ARFs).

The three CW specimens (PomT8PN1, PomT8PN7, PomT8PN8) (Figure 4) have a bimodal distribution of inclusions in an isotropic clayey matrix with high porosity. Pores are mainly oriented parallel to the vessel's surfaces. The small residual inclusions in the clay matrix consist of quartz and micas (muscovite and biotite) (Figure 4). Inclusions in the coarse component (~10%–20%) range from subangular to subrounded and include sparse grains of Ca clinopyroxene, alkali feldspar, plagioclase, and sporadic grains of olivine, rare fragments of volcanic rock that contain crystals of plagioclase and leucite (Figure 4), and ARFs. PomT8PN1 contains speckled calcite in the matrix, whereas in PomT8PN8, there are pores that exhibit calcite coatings.

The three TWW specimens (PomT8PN5, PomT8PN6, PomT8PN9) (Figure 5) exhibit a bimodal distribution of inclusions in a birefringent matrix with high porosity. In two of the three specimens (PomT8PN5, PomT8PN9), there are frequent small, elongated voids oriented parallel to the vessel's surfaces. The small residual inclusions in the clay matrix consist of quartz and micas (mainly muscovite and subordinate biotite) (Figure 5). The inclusions in the coarse component (~20%–25%) are subangular and include sparse grains of Ca clinopyroxene, alkali feldspar, plagioclase, and garnet (Figure 5), scoriae that contain crystals of plagioclase and leucite (Figure 5d), and rare ARFs.

5.2 | Microchemical analyses

EDS was performed for one specimen for each of the three pottery groups due to the marked similarity between the three specimens in each group (FW: PomT8PN3; CW: PomT8PN7; TWW: PomT8PN5). This focused primarily on the assaying of crystals of Ca clinopyroxene, garnet, and leucite, as these crystal analyses were judged to have a significant likelihood of providing significant information regarding geological provenance. The data are presented in Tables 2 and 3.

The clinopyroxenes assayed in all three specimens exhibit a homogeneous composition ($Ca_{51-45}Mg_{42-33}Fe_{17-11}$ in FW; $Ca_{50-48}Mg_{40-35}Fe_{15-13}$ in TWW; $Ca_{50-47}Mg_{41-31}Fe_{19-11}$ in CW) and can be classified as diopside (Figure 6a). In the CaO (wt%) versus MgO (wt%) binary diagram, these analyses follow the trends defined by clinopyroxenes of the CVP (SVVC, continental Phlegraean Fields/Island of Ischia) (Figure 6b). The CW specimen also contains neo-formed calcic clinopyroxene ($Ca_{52-48}Mg_{45-24}Fe_{24-7}$), classifiable as diopside.

The crystals of garnet analyzed in the FW and TWW specimens exhibit high concentrations of both FeO_t (FW: 17.9–20.8 wt%; TWW: 18.2–19.9 wt%) and CaO (FW: 17.9–20.8 wt%; TWW: 18.2–19.9 wt%). These analyses represent a solid solution between different end-members, mainly andradite (60–54 mol% in FW and 59–57 mol% in TWW) and grossular (32–14 mol% in FW and 26–21 mol% in TWW) (calculated following Locock, 2008).

In both the TWW and CW specimens, leucite—frequently altered to analcime—occurs either as a single grain or as an inclusion in a volcanic rock fragment. Values were also obtained for crystals of analcime for one specimen (PomT8PN5 of TWW) and crystals of gehlenite for another specimen (PomT8PN7 of CW).

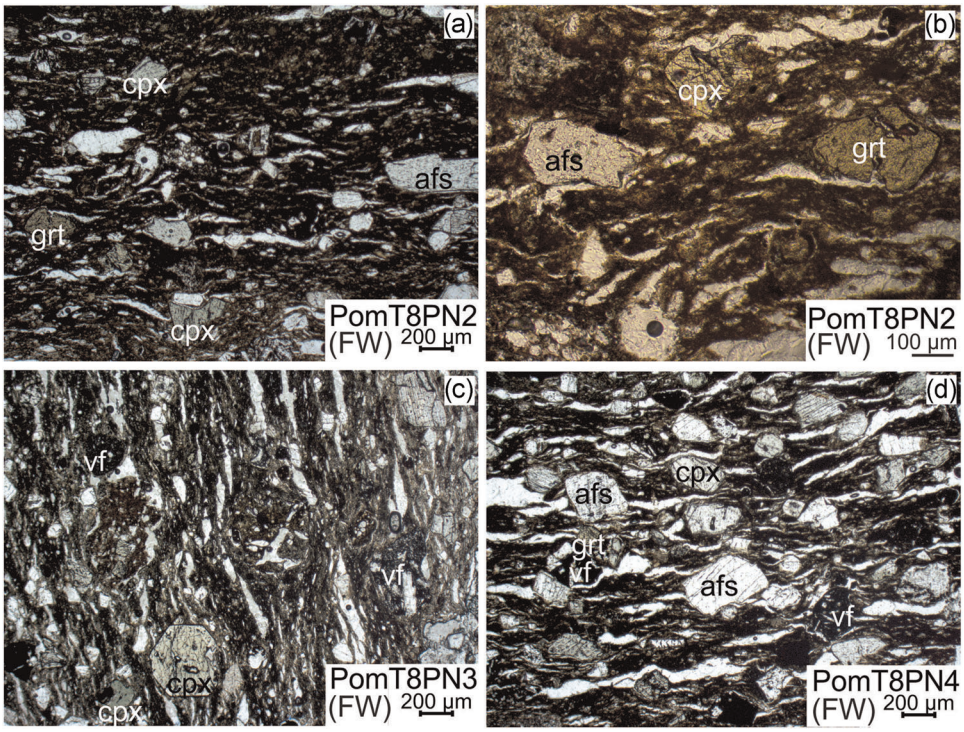

FIGURE 3 Representative thin-section photomicrographs of ferruginous ware (FW) specimens. (a, b) PomT8PN2, (c) PomT8PN3, (d) PomT8PN4. Mineral abbreviations: afs, alkali feldspar; cpx, clinopyroxene; grt, garnet; vf, volcanic fragment (Whitney & Evans, 2010) [Color figure can be viewed at wileyonlinelibrary.com]

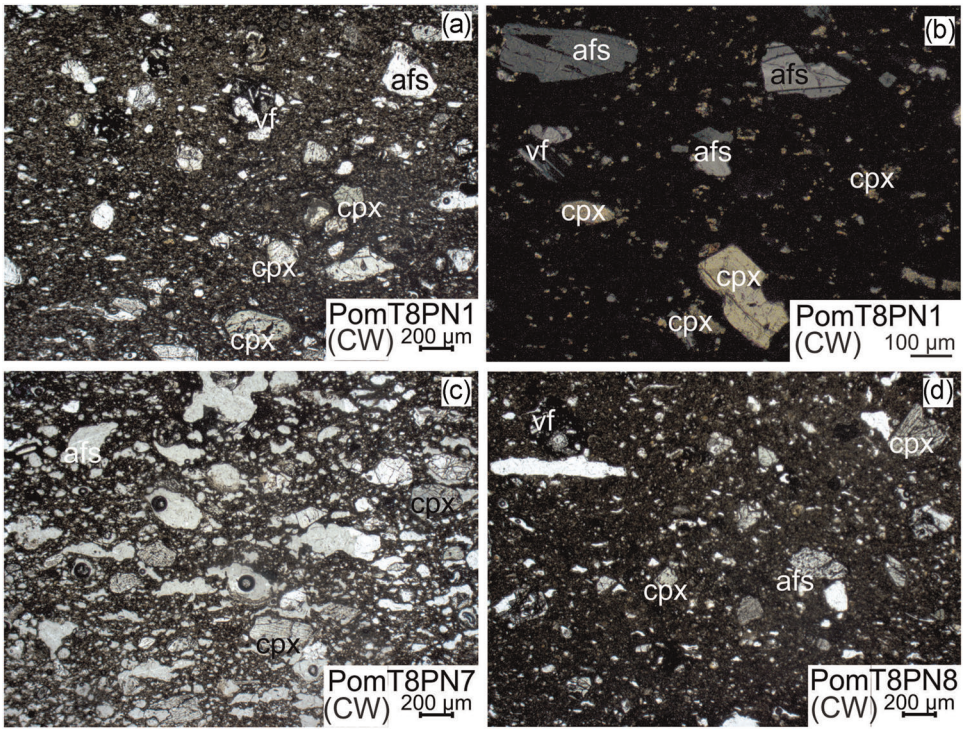

FIGURE 4 Representative thin-section photomicrographs of carbonate ware (CW) specimens. (a, b) PomT8PN1, (c) PomT8PN7, (d) PomT8PN8. Mineral abbreviations: afs, alkali feldspar; cpx, clinopyroxene; grt, garnet; vf, volcanic fragment (Whitney & Evans, 2010) [Color figure can be viewed at wileyonlinelibrary.com]

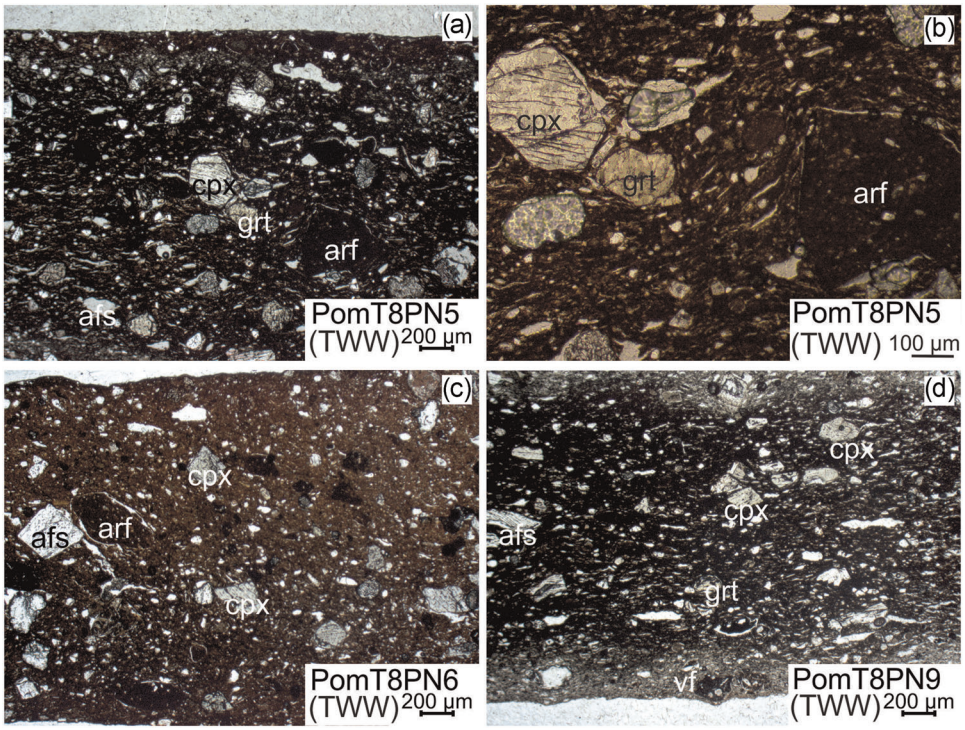

FIGURE 5 Representative thin-section photomicrographs of thin-walled ware (TWW) specimens. (a,b) PomT8PN5, (c) PomT8PN6, (d) PomT8PN9. Mineral abbreviations: afs, alkali feldspar; arf, argillaceous fragment; cpx, clinopyroxene; grt, garnet; vf, volcanic fragment (Whitney & Evans, 2010) [Color figure can be viewed at wileyonlinelibrary.com]

Figure 7 presents a representative BSE image for each of the specimens analyzed. These images underscore the presence of (mainly subrounded) quartz as small residual inclusions in the clay matrix, along with coarse volcanic inclusions (clinopyroxene, garnet, leucite) in PomT8PN3 (FW) (Figure 7a,b) and PomT8PN5 (TWW) (Figure 7e,f). In PomT8PN7 (CW), the quartz grains are subangular, neoformed clinopyroxene is widespread in the matrix (Figure 7c,d), and gehlenite and calcite occur along internal pore surfaces (Figure 7d).

5.3 | Mineralogical and microstructural analyses

A semiquantitative summary of the results obtained by XRPD for all nine specimens is presented in Table 4. Figure 8 presents the diffraction pattern obtained for one specimen for each of the three wares represented (FW: PomPomT8PN3; CW: PomT8PN7; TWW: PomT8PN5).

XRPD indicated the presence of abundant quartz, feldspar, and clinopyroxene in all nine pottery specimens. The three FW specimens contain hematite, with a trace presence of hercynite, mullite, illite/mica, and secondary calcite, the first two of which are firing products. The three CW specimens contain trace amounts of analcime, illite/mica, and gehlenite. The three TWW specimens contain hematite and sporadic illite/mica.

SEM was carried out for the same three specimens for which EDS was performed (FW: PomT8PN3; CW: PomT8PN7; TWW: PomT8PN5). Figure 9 presents a representative image of the fracture surface for each of the specimens analyzed. Both PomT8PN3 (FW) and PomT8PN7 (CW) exhibit continuous vitrification, whereas PomT8PN5 (TWW) displays extensive, though non-continuous vitrification (Table 4).

5.4 | XRF analysis

The data obtained by XRF for all nine specimens are presented in Table 5.

Both the FW and TWW specimens display low values for CaO (FW: 3.1–5 wt%; TWW: 2.6–2.7 wt%) and high values for SiO_2 (FW: 57.6–59.5 wt%; CW: 59.9–60.8 wt%), whereas the CW samples demonstrate high values for CaO (14.4–15.8 wt%) and low values for SiO_2 (53.2–54.2 wt%). The Al_2O_3 values are slightly higher in the FW and TWW specimens (FW: 19.7–21.2 wt%; TWW: 19.5–20.1 wt%) than in the CW specimens (15.4–16.3 wt%). The MgO concentration is similar in all three ceramic groups (FW: 2–2.8 wt%; TWW: 2.9–3 wt%; CW: 3.2–3.4 wt%), as are those for Na_2O (<1.3 wt%) and P_2O_5 (<0.2 wt%).

The FW specimens exhibit higher values for Zr (431–499 ppm), compared with the CW specimens (127–168 ppm) and the TWW specimens (235–281 ppm), lower values for Cr (105–128 ppm), compared with the CW specimens (132–166 ppm) and the FW specimens (174–190 ppm), and lower values also for Ni (33–42 ppm), compared with the CW specimens (61–77 ppm) and the TWW specimens (63–76 ppm). The CW specimens display higher values for

TABLE 2 Representative compositions of Ca clinopyroxenes analyzed in the PomT8PN3 (FW), PomT8PN7 (CW), and PomT8PN5 (TWW) samples

	FW (Group 1)						CW (Group 2)			
Naples ware	PomT8PN3	PomT8PN3	PomT8PN3	PomT8PN3	PomT8PN3	PomT8PN3	PomT8PN7	PomT8PN7	PomT8PN7	PomT8PN7
Naples ID	cpx	cpx	cpx	cpx	cpx	cpx	cpx	cpx	cpx neof	cpx neof
SiO_2 (wt%)	46.6	47.1	49.8	49.8	49.4	48.3	45.8	49.8	49.4	51.1
TiO_2	1.02	1.11	0.29	1.16	0.96	1.36	1.12	0.96	1.01	1.23
Al_2O_3	8.26	6.60	4.03	3.84	3.83	5.75	6.51	3.90	6.43	6.47
MgO	11.0	12.8	12.9	14.6	14.6	13.5	10.4	14.3	10.1	9.43
CaO	23.7	23.6	23.3	21.6	21.9	21.9	23.1	22.8	22.7	22.6
MnO	0.32	0.18	0.59	0.55	0.11	0.26	0.09	0.28	0.00	0.31
FeO	9.87	7.46	8.82	7.22	8.22	6.51	10.8	7.00	9.18	9.56
Na_2O	0.18	0.21	0.45	0.25	0.14	0.26	0.35	0.19	0.10	0.42
Total	101.0	99.1	100.1	99.0	99.2	97.9	98.2	99.2	99.0	101.1
Normalized at six oxygens										
Si (apfu)	1.730	1.763	1.850	1.859	1.845	1.824	1.755	1.855	1.883	1.911
Ti	0.029	0.031	0.008	0.033	0.027	0.039	0.032	0.027	0.029	0.035
Al	0.361	0.291	0.176	0.169	0.168	0.256	0.294	0.171	0.289	0.285
Mg	0.608	0.715	0.712	0.815	0.811	0.762	0.596	0.797	0.571	0.526
Ca	0.944	0.947	0.928	0.864	0.878	0.886	0.946	0.909	0.928	0.905
Mn	0.010	0.006	0.019	0.017	0.003	0.008	0.003	0.009	0.000	0.010
Fe	0.306	0.233	0.274	0.225	0.257	0.206	0.348	0.218	0.292	0.299
Na	0.013	0.015	0.032	0.018	0.010	0.019	0.026	0.014	0.008	0.030
Total	4	4	4	4	4	4	4	4	4	4
Ca	51	50	48	45	45	48	50	47	52	52
Mg	33	38	37	42	42	41	31	41	32	30
Fe	17	13	15	13	13	11	19	12	16	18

	CW (Group 2)					TWW (Group 3)				
Naples ware	PomT8PN7	PomT8PN7	PomT8PN7	PomT8PN7	PomT8PN7	PomT8PN5	PomT8PN5	PomT8PN5	PomT8PN5	PomT8PN5
Naples ID	cpx neof	cpx neof	cpx neof	cpx neof	cpx neof	cpx	cpx	cpx	cpx	cpx
SiO_2 (wt%)	52.1	52.5	42.7	51.8	47.7	50.0	49.3	49.1	48.3	49.6
TiO_2	0.76	0.14	1.97	1.01	1.09	0.59	1.18	0.97	1.43	1.17

TABLE 2 (Continued)

Naples ware	CW (Group 2)					TWW (Group 3)				
	PomT8PN7	PomT8PN7	PomT8PN7	PomT8PN7	PomT8PN7	PomT8PN5	PomT8PN5	PomT8PN5	PomT8PN5	PomT8PN5
Naples ID	cpx neof	cpx neof	cpx neof	cpx neof	cpx neof	cpx	cpx	cpx	cpx	cpx
Al_2O_3	5.10	2.53	9.34	8.50	5.25	2.58	5.08	5.38	5.67	4.86
MgO	9.89	16.1	7.7	8.7	13.3	12.9	13.6	11.7	13.4	13.9
CaO	22.4	23.9	22.9	20.3	22.9	23.4	22.6	23.3	22.3	22.2
MnO	0.20	0.26	0.39	0.14	0.26	0.70	0.32	0.40	0.11	0.24
FeO	8.71	4.06	12.97	9.12	6.42	8.45	7.84	8.24	7.72	8.15
Na_2O	-	0.03	0.45	0.18	0.05	0.55	0.12	0.67	0.20	0.17
Total	99.2	99.5	98.4	99.8	96.9	99.2	100.0	99.7	99.1	100.3
Normalized at six oxygens										
Si (apfu)	1.988	1.928	1.653	1.964	1.824	1.876	1.829	1.836	1.810	1.836
Ti	0.022	0.004	0.057	0.029	0.031	0.017	0.033	0.027	0.040	0.032
Al	0.229	0.110	0.426	0.380	0.236	0.114	0.222	0.237	0.250	0.212
Mg	0.562	0.880	0.447	0.494	0.756	0.722	0.755	0.650	0.746	0.767
Ca	0.914	0.943	0.950	0.825	0.935	0.943	0.898	0.931	0.893	0.880
Mn	0.007	0.008	0.013	0.005	0.008	0.022	0.010	0.013	0.004	0.008
Fe	0.278	0.125	0.420	0.289	0.205	0.265	0.244	0.257	0.242	0.252
Na	-	0.002	0.034	0.013	0.004	0.040	0.008	0.049	0.015	0.012
Total	4	4	4	4	4	4	4	4	4	4
Ca	52	48	52	51	49	48	47	50	47	46
Mg	32	45	24	31	40	37	40	35	40	40
Fe	16	7	24	18	11	15	13	15	13	14

Abbreviations: apfu, atoms per formula unit; cpx, clinopyroxene; cpx neof, neoformed clinopyroxene; CW, carbonate ware; FW, ferruginous ware; TWW, thin-walled ware.

TABLE 3 Representative compositions of garnet, leucite, calcite, and gehlenite analyzed in the PomT8PN3 (FW), PomT8PN7 (CW), and PomT8PN5 (TWW) samples

Naples ware	FW (Group 1)			CW (Group 2)							TWW (Group 3)					
	PomT8P-N3	PomT8P-N3	PomT8P-N3	PomT8P-N7	PomT8P-N7	PomT8P-N7	PomT8P-N7	PomT8P-N7	PomT8P-N7	PomT8P-N7	PomT8P-N5	PomT8P-N5	PomT8P-N5	PomT8P-N5	T8PN5	PomT8PN5
Naples ID	grt	grt	grt	cal	cal	cal	cal	cal	gh	gh	grt	grt	lct	anl	anl	anl
SiO_2 (wt%)	35.0	35.4	34.8	-	-	-	-	-	30.9	33.4	34.98	35.98	57.0	51.7	54.7	54.9
TiO_2	2.60	1.87	4.14	-	-	-	-	-	0.44	2.53	3.31	3.38	0.1	0.1		0.1
Al_2O_3	7.96	9.15	6.19	-	-	-	-	-	18.0	17.1	8.12	7.57	23.2	20.5	22.0	21.9
Cr_2O_3	0.07	0.05	-	-	-	-	-	-	-	-	-	-	-	-	-	-
V_2O_3	0.05	0.15	0.54	-	-	-	-	-	-	-	-	0.15	-	-	-	-
FeO	19.3	17.9	20.8	-	0.18	-	-	-	7.54	14.74	18.2	19.9	0.14	0.14	0.37	0.57
MnO	1.58	1.37	0.82	-	-	-	0.33	0.40	0.18	0.27	1.17	1.23	-	-	-	-
MgO	0.33		0.35	0.77	1.94	0.72	1.90	6.63	3.67	4.83	0.13	0.37	0.08	0.26	0.11	0.11
CaO	31.1	31.2	31.8	51.54	50.88	48.10	51.08	44.72	38.8	25.1	32.6	32.3	0.03	0.39	0.27	0.24
Na_2O	0.07	0.13	-	0.03	0.24	0.65	0.05	0.16	0.26	-	0.02	0.13	0.44	6.01	9.24	8.30
K_2O	-	-	-	0.06	-	0.10	0.01	-	0.11	-	-	-	20.6	1.6	1.2	1.2
SrO	-	-	-	0.17	0.21	0.36	0.07	-	-	-	-	-	-	-	-	-
BaO	-	-	-	-	0.31	-	-	0.39	-	-	-	-	-	-	-	-
Total (calc.)	98.1	97.2	99.6	52.6	53.8	49.9	53.4	52.3	99.9	98.0	98.5	101.0	101.6	80.7	87.9	87.5
Recalculated (wt%)																
Final FeO	1.86	2.09	3.14								1.57	2.15				
Final Fe_2O_3	19.4	17.5	19.7								18.5	19.7				
Final MnO	1.58	1.37	0.82								1.17	1.23				
Final Mn_2O_3	-	-	-								-	-				
Total	100.0	99.0	101.5								100.4	103.0				
End-members																
Schorlomite-Al	6.8%	4.7%	8.5%								7.8%	7.0%				
Morimotoite	1.1%	0.1%	8.4%								4.3%	4.1%				
NaTi garnet	0.6%	1.0%	-								0.2%	1.0%				
Goldmanite	0.2%	0.5%	1.8%								-	0.5%				
Uvarovite	0.2%	0.2%	-								-	-				
Spessartine	3.7%	3.2%	1.9%								2.7%	2.8%				
Pyrope	1.3%	-	1.4%								0.5%	1.5%				

TABLE 3 (Continued)

Naples ware	FW (Group 1)			CW (Group 2)							TWW (Group 3)					
	PomT8P-N3	PomT8P-N3	PomT8P-N3	PomT8P-N7	PomT8P-N7	PomT8P-N7	PomT8P-N7	PomT8P-N7	PomT8P-N7	PomT8P-N7	PomT8P-N5	PomT8P-N5	PomT8P-N5	PomT8P-N5	T8PN5	PomT8PN5
Naples ID	**grt**	**grt**	**grt**	**cal**	**cal**	**cal**	**cal**	**cal**	**gh**	**gh**	**grt**	**grt**	**lct**	**anl**	**anl**	**anl**
Almandine	3.9%	4.8%	4.3%								2.1%	3.4%				
Grossular	22.7%	31.6%	13.6%								25.7%	20.8%				
Andradite	59.6%	54.0%	60.2%								56.7%	58.9%				
Remainder	0.0%	0.0%	0.0%								0.0%	0.0%				
Total	100%	100%	100%								100%	100%				
Quality index	Superior	Superior	Superior								Superior	Superior				

Note: The garnet end-members are calculated with Excel spreadsheet of Locock (2008).

Abbreviations: anl, analcime; cal, calcite; gh, gehlenite; grt, garnet; lct, leucite (Whitney and Evans, 2010); CW, carbonate ware; FW, ferruginous ware; TWW, thin-walled ware.

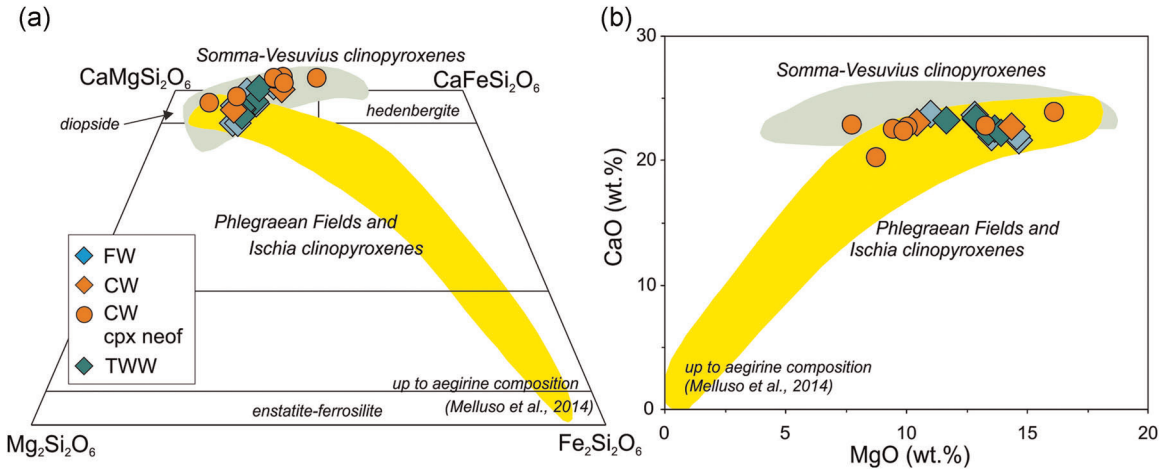

FIGURE 6 (a) Classification of clinopyroxenes from the FW, CW, and TWW samples according to Morimoto (1988). (b) Compositional variation is shown in the CaO (wt%) versus MgO (wt%) diagram. Main fields from Campania volcanic districts are reported for comparison (Melluso et al., 2012, 2014, and references therein, and Prof. Melluso, unpublished data). cpx neof, neoformed clinopyroxene; CW, carbonate ware; FW, ferruginous ware; TWW, thin-walled ware [Color figure can be viewed at wileyonlinelibrary.com]

Sr (327–432 ppm), compared with the TWW specimens (199–208 ppm) and the FW specimens (267–358 ppm). The values for Rb are similar in the FW and TWW specimens (FW: 200–220 ppm; TWW: 183–202 ppm) and lower in the CW specimens (128–142 ppm).

Figure 10 presents a set of six binary diagrams that illustrate some of the main chemical features that differentiate the three groups of pottery characterized. This figure also displays colored zones that represent the compositional fields associated with various classes of archaeological pottery of certain or likely Campanian origin manufactured with both low-CaO (CaO < 6 wt% after Maniatis & Tite, 1981) and high-CaO clayey raw materials. The three groups are clearly distinct from each other and generally show a good homogeneity (Figure 10), apart from a sample of FW (PomT8PN4) that slightly differs from others in the same group.

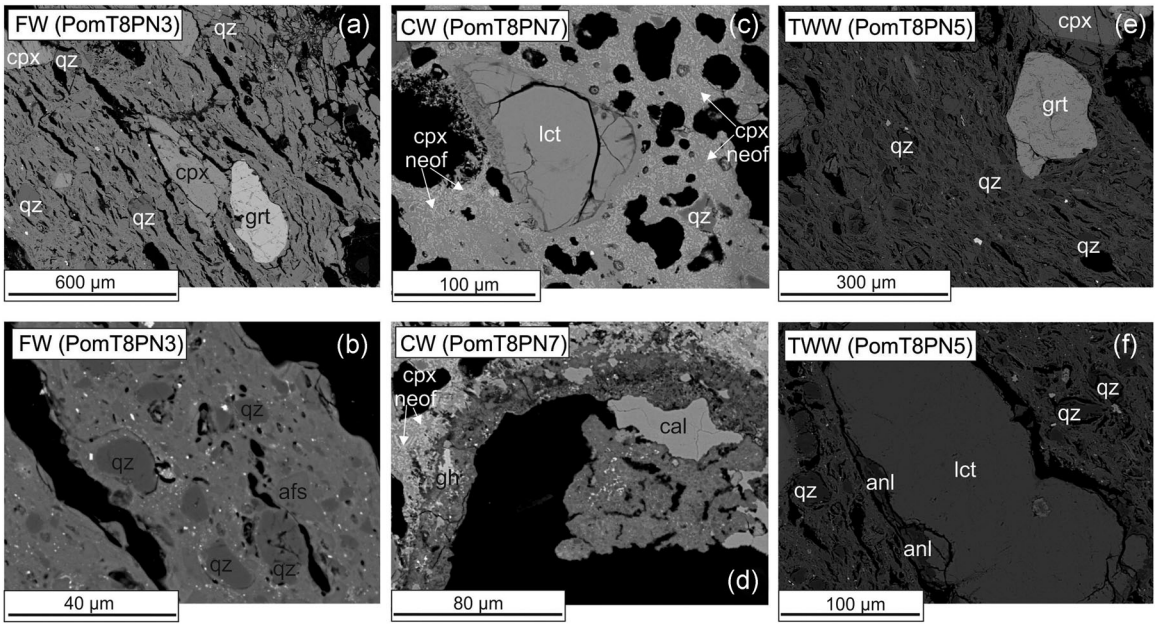

FIGURE 7 Representative backscattered electron images of Pompeii samples. Garnet and clinopyroxene crystals (a) in a ceramic matrix with rounded quartz inclusions (b) in PomT8PN3 sample (FW); leucite crystals set in a ceramic matrix in which are observed tiny light gray crystals of neoformed Ca clinopyroxene (c) and a pore filled by calcite where gehlenite exists along the border (d) in PomT8PN7 sample (CW); garnet (e) and leucite border by analcime (f) in PomT8PN5 sample (TWW) set in a matrix with rounded quartz. afs, alkali feldspar; anl, analcime; cal, calcite; cpx, clinopyroxene; cpx neof, neoformed clinopyroxene; gh, gehlenite; grt, garnet; lct, leucite; qz, quartz; vf, volcanic fragment (Whitney & Evans, 2010); CW, carbonate ware; FW, ferruginous ware; TWW, thin-walled ware

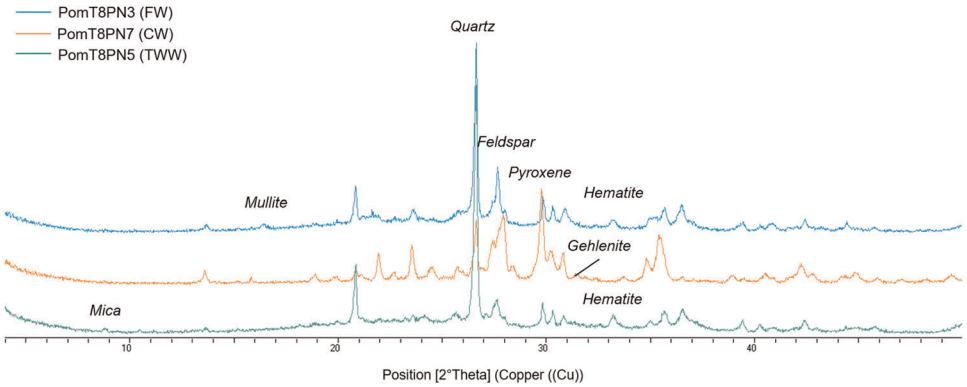

FIGURE 8 XRPD patterns of PomT8PN3 (FW), PomT8PN7 (CW), and PomT8PN5 (TWW) samples. CW, carbonate ware; FW, ferruginous ware; TWW, thin-walled ware; XRPD, X-ray powder diffraction [Color figure can be viewed at wileyonlinelibrary.com]

5.5 | Sr and Nd isotope geochemistry

The characterization of Sr and Nd isotopes represents an interesting, though little-explored method that indicates the potential of radiogenic isotope analysis for determining the provenance of ancient ceramics (De Bonis et al., 2018; Kibaroğlu et al., 2019; Renson, Jacobs, et al., 2013; Renson, Martínez-Cortizas, et al., 2013; Renson et al., 2016). The analyses conducted by the Naples group (De Bonis et al., 2018; Morra et al., 2020) tested the use of Sr and Nd isotopes for ceramic replicas made with local raw materials and archaeological pottery manufactured in the GBNR. The obtained results clearly reveal the following findings: (1) the fired test tiles display no significant variation from the isotopic ratios of their respective unfired synthetic mixtures, indicating that the heating process does not affect the isotopic composition; (2) all fired and unfired test pieces diverge only very slightly from the theoretical mixing line extending from the Ischia clay to the volcanic sand AQM2, proving that artificial mixing of raw materials affects the isotopic signature in a predictable way, depending on the proportions of the end-members; and (3) both the sand and clay analyzed have an isotopic fingerprint that relates strictly to their geological origin (De Bonis et al., 2018).

Following the results obtained in De Bonis et al. (2018), the Sr–Nd method was applied for the three ceramic groups (FW, CW, and TWW). The results are presented in Table 5 and shown in Figure 11.

This figure reports two new elaborated theoretical mixing lines between the same volcanic sand (AQM2), one extending to the RUF1 (Rufoli di Ogliara; orange line) clay and the other to the PDS1 (Piano di Sorrento; green line) clay, and one mixing line between SO1 (Sant'Agnello) and AGE1 (Agerola; blue line) clays. These mixing lines are of considerable interest due to the fact that PomT8PN7—the specimen in the CW group—plots along the line extending from AQM2 to RUF1 (orange line), PomT8PN5—the specimen in the TWW group—falls only slightly above the line extending from AQM2 to PDS1 and well away from the first line (green line), whereas PomT8PN3 and PomT8PN4—specimens in the FW group—plot along the line extending from SO1 and AGE1 (blue line). These results indicate that the CW and TWW vessels were manufactured from a paste consisting of a mixture of one of these two clays and volcanic sand temper from the CVP, whereas the FW was likely manufactured with a mixture of two volcanic-derived clays.

6 | DISCUSSION

The multianalytical approach is very useful for the development of our knowledge of pottery manufactured at Pompeii, confirming the attribution of the nine pottery specimens from the Tower 8/Porta di Nola middens to three different classes/wares characterized by compositionally distinct ceramic bodies.

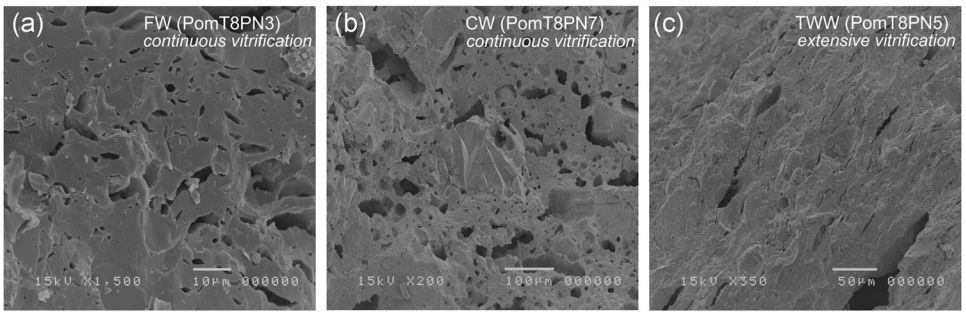

FIGURE 9 Secondary electron scanning electron microscopy images of freshly fractured samples. (a, b) Continuous vitrification in PomT8PN3 (FW) and PomT8PN7 (CW); and (c) extensive vitrification in PomT8PN5 (TWW). CW, carbonate ware; FW, ferruginous ware; TWW, thin-walled ware

The program of analysis also confirms the initial inferences made regarding the likely set of raw materials and paste preparation practices involved in the manufacture of the CW (Group 2) specimens. XRF indicates that all three specimens in this group contain high concentrations of CaO compatible with the use of a high-calcium clay of marine origin. OM, XRPD, and EDS show that all three specimens contain a coarse volcanic inclusion component consisting of minerals and rock fragments. Volcanic materials of this kind do not occur naturally in the high-calcium marine clays that outcrop mainly along Apennine Chain, and it can thus be safely assumed that the coarse inclusion component represents temper, that is, coarse material deliberately added to the ceramic paste by the potters rather than a natural component of the clay. In general terms, the fabric of the CW specimens corresponds with that of compositional fabric group 1d that Mannoni defined in a program of OM involving pottery recovered in excavations carried out at the Casa dei Fiori/Casa del Cinghiale (VI.5.9.10/19) at Pompeii (Mannoni, 1984; Peña & McCallum, 2009b).

The presence of leucite crystals in some of the volcanic fragments in the CW specimens points to an origin for the tempering material employed in their manufacture in one or more formations belonging to the SVVC. The absence of carbonate rock fragments in the coarse inclusion component suggests that this material was neither a Sarno sediment nor beach sand obtained from a location either at the mouth of the Sarno River or along the shore of the Bay of Naples to the south (Morra et al., 2013). In light of these observations, it seems likely that the coarse inclusion component in these specimens consists of beach sand obtained at a location somewhere to the north of the mouth of the Sarno River, presumably at no great distance from Pompeii.

As noted in the preceding section, TIMS of one of the CW specimens yielded a Sr–Nd isotope ratio that falls along the mixing line extending from the specimen of Acquamorta beach sand to a specimen of marine clay from the Rufoli di Ogliara outcrop (Figure 11). This suggests that the CW vessels were manufactured with clay from an Apennine wedge-top deposit of the Altavilla Group (De Bonis et al., 2013; Vitale & Ciarcia, 2018), probably obtained either from this same outcrop or from the deposit of the Montecorvino Rovella outcrop. The same results supporting the exploitation of these deposits, also complemented with paleontological constraints, were obtained by Grifa et al. (2021a) for the high-CaO thin-walled ware found in the *Via dei Sepolcri* workshop. The chemical data obtained for the CW specimens by XRF were subjected to multivariate statistical analysis, with the results providing general confirmation of these inferences (Figure 12a). PCA showed that 96% of the cumulative variance of the sample population was explained here with the first six components (Nb, Cr, K_2O, Sc, Na_2O, Y). The resulting HCA dendrogram (Euclidean distance and average linkage method) indicates the existence of a high level of chemical homogeneity among the three CW specimens, confirming their compositional integrity as a production group and a general chemical similarity between these and clay samples from the Apennine wedge-top basin deposits, including those that outcrop at Rufoli di Ogliara and Montecorvino Rovella (samples labeled RUF and MCR; Figure 12a).

Contemporary ceramic producers at both Rufoli di Ogliara and Montecorvino Rovella state that the clay that they extract from the Apennine wedge-top basin deposits that outcrop at these two locations has a tendency to crack during drying due to its high rate of shrinkage, and they accordingly mix it with coarse material of various kinds when preparing their paste to counteract this phenomenon (Peña & Kane, 2016). Pompeiian potters likely added volcanic sand temper to the paste employed for the manufacture of CW pottery for this same purpose.

As previously noted, the location of the outcrop of Apennine wedge-top basin clay at Rufoli di Ogliara raises the possibility that in Roman times, material from this source was distributed by sea via the port at Salernum to distant coastal settlements, such as Pompeii (see also Grifa et al., 2021a). The shortest route sailing distance for a coasting voyage from Salernum to Pompeii would have been ca. 36.5 nautical miles (67.6 km) long (http://www.andiamociavela.it/files/Distanze-di-navigazione-costiere-Sorrentina-e-Amalfitana.jpg). If we assume that in many cases, a voyage of this kind could have been completed at an average speed of between 2 and 4 knots (3.7–7.4 km/h) (Casson, 1951; Pryor, 1989), we can estimate a one-way travel time of between 9.125 and 18.25 h. Although these figures represent only rough approximations, they offer a useful idea of the distance and travel time involved in completing a sailing journey from Salernum to Pompeii, and thus the scale of the transport costs entailed for Pompeiian potters in obtaining this material.

The interpretation of the analytical results regarding the FW (Group 1) and TWW (Group 3) specimens is less straightforward. OM reveals that all six specimens possess a bimodal distribution of inclusions, with a fine fraction representing the natural component of the clay body, consisting of small grains of rounded quartz and detrital plates of muscovite, and a coarse component, either added as a temper or a natural component, consisting of medium to large volcanic grains (both mineral and rock fragments). In both groups, the presence of garnet and leucite-bearing scoriae in the coarse component indicates an origin for this material in the SVVC. This conclusion is supported by the results of EDS, which obtained values for the garnets assayed that are typical for the SVVC (Scheibner et al., 2007 and Prof. Melluso, unpublished data). Both of these groups can be assigned to Mannoni's Fabric Group 1a (Mannoni, 1984; Peña & McCallum, 2009b).

The results of XRF confirm that the specimens in both groups were manufactured with a low-CaO clay. The TWW specimens are more homogenous than FW specimens, and they exhibit non-overlapping ranges of values for most of the major and trace elements measured. This may suggest the use of two distinct low-CaO clayey raw materials. To identify the possible nature and geographic origin of these materials, we subjected the chemical data for these obtained by XRF to HCA. In this case, PCA showed that 95% of the cumulative variance of the sample population was explained with the first seven components (TiO_2, Nb, K_2O, Rb, MgO, Al_2O_3, Ni). The

TABLE 4 Mineralogical analysis (XRPD) and equivalent firing temperatures of pottery samples

Naples ware	Naples ID	Quartz	Feldspar	Pyroxene	Hematite	Fe^{2+} oxides	Gehlenite	Mullite	Analcime	Illite/mica	Calcite	Firing atmosphere	Vitrification stage	Temperature (°C)
FW (Group 1)	PomT8PN2	xxxx	xxx	xx	x	-	-	-	-	Traces	Traces	Reducing and oxidizing conditions	-	750–950
	Pomt8PN3	xxxx	xxx	xx	x	x (Hercynite)	-	Traces	-	-	-		CV	>1000
	PomT8PN4	xxxx	xxx	xx	x	-	-	-	-	x	-		-	750–900
CW (Group 2)	PomT8PN1	xxx	xxx	xxxx	-	-	-	-	-	-	-	Oxidizing conditions	-	>950
	PomT8PN7	xx	xxx	xxxx	-	-	x	-	-	-	-		CV	1000–1050
	PomT8PN8	xxxx	xxx	xxx	-	-	-	-	Traces	Traces	-		-	<950
TWW (Group 3)	PomT8PN5	xxxx	xx	xx	x	-	-	-	-	Traces	-	Oxidizing conditions	V	850–950
	PomT8PN6	xxxx	xx	xx	x	-	-	-	-	Traces	-		-	750–950
	PomT8PN9	xxxx	x	xx	x	-	-	-	-	-	-		-	900–1000

Note: xxxx = very abundant; xxx = abundant; xx = frequent; x = scarce. Vitrification stages observed at SEM were also reported (Maniatis & Tite, 1981).

Abbreviations: CV, continuous vitrification; SEM, scanning electron microscopy; V, extensive vitrification; XRPD, X-ray powder diffraction.

resulting HCA dendrogram indicates the existence of a high level of chemical homogeneity among the three specimens belonging to each of the two groups, confirming the compositional integrity of these as production groups (Figure 12b).

The TWW (Group 3) specimens show a good affinity with a set of clays composed of specimens from several widely separated locales at a considerable distance from Pompeii, including three specimens of alluvial clay (CET2, PMV2, VEL1) and seven specimens of so-called varicolored clays of marine origin (BS1, BS2, SMV1, SCP1, CPR2, SQ1, PDS1) (see Table S2 for geologic details). Interestingly, the TWW specimens are clustered close to the PDS1 clay specimen. This clay, which was collected on a hilltop in the Piano di Sorrento area (Figure 1c), can be attributed to olistostromes and olistoliths composed of varicolored clays that belong to the Castelvetere wedge-top deposits (Vitale & Ciarcia, 2018). This association is amplified by the results of the program of isotopic analysis. Here, the TWW specimen analyzed (PomT8PN5) exhibited an Sr isotope ratio that was substantially higher than that obtained for the other pottery specimens analyzed (Figure 11). The PDS1 clay specimen exhibited a more radiogenic Sr isotope ratio, and the theoretical mixing curve extending from the AQM2 volcanic sand to this clay (Figure 11; green line) indicates that this pottery specimen may have been manufactured from a combination of Piano di Sorrento marine clay or a similar clay and SVVC volcanic sand, with the latter comprising ca. 20% of the paste, a result compatible with the observations made in the OM of PomT8PN5.

The FW specimens, in contrast, display a general degree of similarity, based on the elemental composition, with clay specimens obtained from argillified pyroclastic deposits, with a particular affinity with two specimens from deposits of this kind, one specimen from the Sant'Agnello area on the Sorrentine Peninsula, referred to in Section 3, and the other specimen from a source near Lettere, in the Monti Lattari, ca. 8.5 km to the southeast of Pompeii (Figure 1c).

As discussed below, four passages in the ancient Greek and Latin literature [*Anthologia Graeca* (11.27); Pliny *Historia Naturalis* (31.60); Martial *Epigrammata* (13.110; 14.102)] indicate that clay obtained in the environs of Surrentum was widely employed for the manufacture of pottery during the first-century CE (Peña & McCallum, 2009b). This territory would have embraced both the Piano di Sorrento area and the Sant'Agnello area, and thus the sources of both clay specimen PDS1 and clay specimen SO1 located <5 km from each other (Figure 1c). If, as just noted, the results of the program of analysis (HCA and XRF data) suggest that Piano di Sorrento clay or a clay similar to this was employed for the manufacture of the TWW group, they also raise the possibility that Sant'Agnello clay or a clay similar to this was employed for the manufacture of the FW group. Specifically, the petrographic features of the FW specimens are generally similar to those of specimen SO1, a volcanic-derived clay that is used by contemporary brick and tile makers at Maiano. This material is characterized by frequent coarse rock fragments and mineral grains typical of SVVC formations along with grains derived from the nearby arenaceous (quartz and sandstone) and carbonate formations reworked by landslides (De Bonis et al., 2014).

TABLE 5 New chemical analysis (XRF) of major oxides (wt%), trace elements (ppm), and LOI (wt%) of FW, CW, and TWW specimens and PDS1 and AGE1 clays, with new $^{87}Sr/^{86}Sr$ and $^{143}Nd/^{144}Nd$ isotope data of PomT8PN3 (FW), PomT8PN4 (FW), PomT8PN7 (CW), PomT8PN5 (TWW), PDS1, AGE1 and RUF1

	FW (Group 1)			CW (Group 2)			TWW (Group 3)			Clayey raw materials				Raw clay	Local volcanic sand
	PomT8P-N2	PomT8P-N3	PomT8P-N4	PomT8P-N1	PomT8P-N7	PomT8P-N8	PomT8P-N5	PomT8P-N6	PomT8P-N9	PDS1	AGE1	RUF1[a]	SO1[a]	IS6[a]	AQM/AQM2[b,c]
SiO_2 (wt%)	58.7	59.5	57.6	53.5	53.2	54.2	60.3	59.9	60.8	60.6	57.7	54.3	58.0	60.0	61.2
TiO_2	1.00	1.02	1.02	0.81	0.82	0.81	1.11	1.07	1.12	1.26	1.04	0.77	0.90	0.77	0.66
Al_2O_3	21.2	21.0	19.7	15.4	15.6	16.3	19.9	20.1	19.5	22.7	25.9	15.0	24.2	15.8	16.3
Fe_2O_3	8.18	7.99	8.36	7.17	7.03	6.77	8.84	8.70	8.73	7.02	8.61	6.59	7.38	6.1	4.98
MnO	0.21	0.12	0.15	0.13	0.12	0.11	0.12	0.11	0.13	0.03	0.14	0.07	0.19	0.14	0.12
MgO	2.08	2.03	2.76	3.43	3.19	3.21	2.89	2.98	2.97	3.07	2.27	3.94	1.86	2.94	1.93
CaO	3.67	3.11	5.03	15.7	15.8	14.4	2.65	2.64	2.70	1.33	0.94	15.7	2.57	9.70	4.29
Na_2O	1.11	1.02	1.27	0.86	0.86	1.04	0.60	0.60	0.54	0.12	0.19	0.70	0.79	0.86	3.25
K_2O	3.46	3.91	3.64	2.72	2.97	2.81	3.29	3.57	3.20	3.71	2.90	2.83	4.04	3.47	7.08
P_2O_5	0.12	0.11	0.19	0.19	0.19	0.23	0.13	0.13	0.12	0.07	0.05	0.14	0.14	0.15	0.18
LOI	0.26	0.25	0.29	0.16	0.18	0.16	0.19	0.19	0.19	11.1	12.1	17.9	11	12.1	1.73
Rb (ppm)	220	219	200	142	128	132	202	183	191	187	256	144	175	160	193
Sr	282	267	358	432	420	327	199	208	200	171	183	444	396	234	507
Y	36	36	48	27	28	23	36	32	34	40	137	30	40	27	19
Zr	495	499	431	159	168	127	281	235	264	223	680	122	359	263	245
Nb	52	52	48	18	18	16	30	27	28	36	60	14	54	27	35
Ba	750	660	908	422	432	364	493	534	485	381	552	255	1010	369	712
Cr	115	105	128	166	141	132	176	174	190	189	81	133	34	74	-
Ni	35	33	42	77	61	64	63	76	68	55	105	44	26	41	5
Sc	22	21	24	24	26	23	26	28	27	23	19	27	10	18	6
V	220	206	229	187	182	146	243	199	232	176	171	-	-	-	-
La	92	78	125	40	50	46	77	64	56	75	363	-	-	-	-
Ce	194	168	222	81	72	86	122	119	110	132	315	-	-	-	-
$^{87}Sr/^{86}Sr$		0.708762	0.709607		0.709863		0.712442			0.716450	0.711430	0.710404	0.70783(d)	0.71114	0.706945
$^{143}Nd/^{144}Nd$		0.512377	0.512349		0.512217		0.512180			0.512007	0.512261	0.512124	0.51245(d)	0.51226	0.51251

Note: Data from (a) De Bonis et al. (2013); (b) Morra et al. (2013); (c) De Bonis et al. (2014).

Abbreviations: CW, carbonate ware; FW, ferruginous ware; LOI, loss on ignition; TWW, thin-walled ware; XRF, X-ray fluorescence.

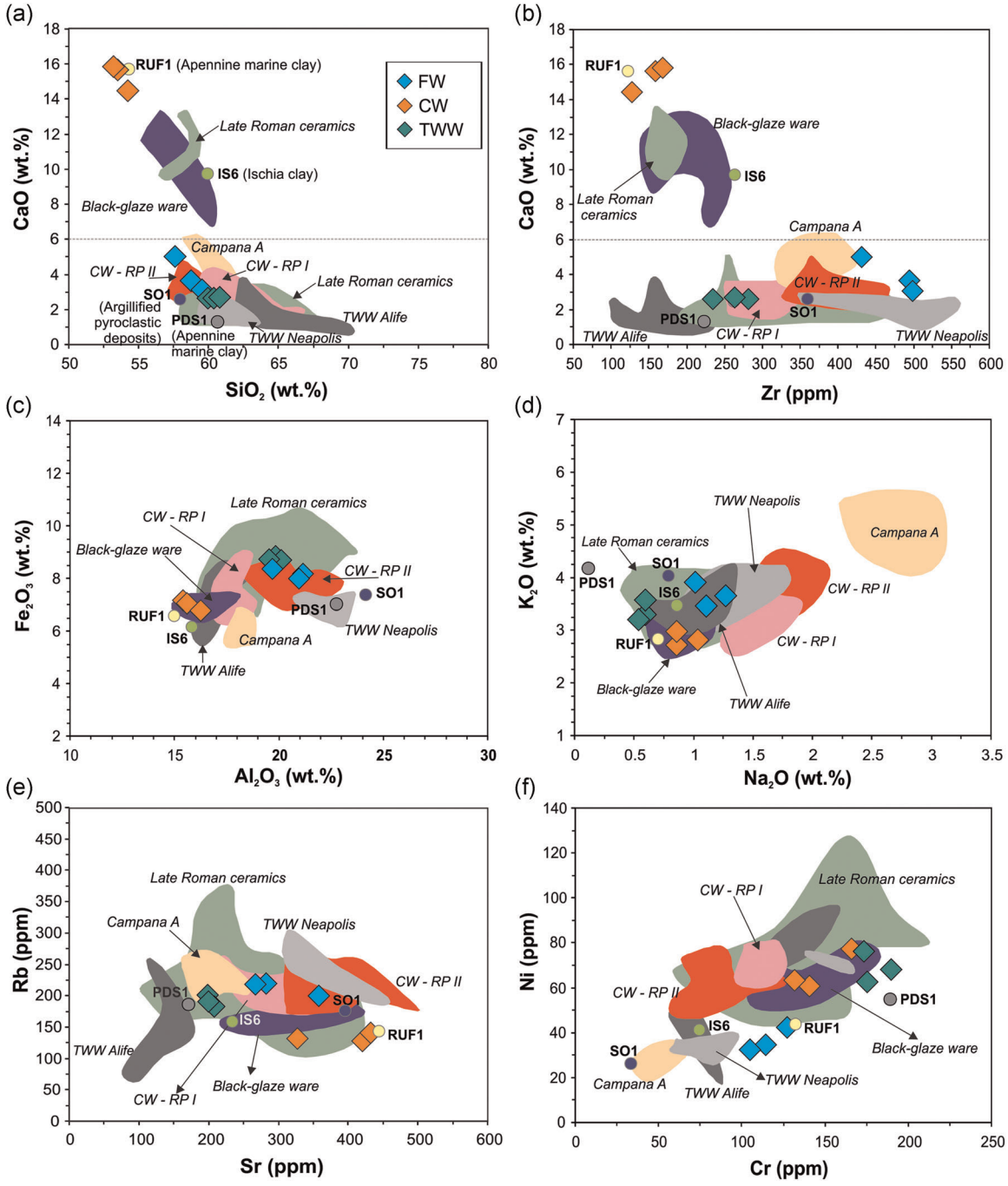

FIGURE 10 Representative binary diagrams for the FW, CW, and TWW specimens. (a) CaO (wt.%) vs. SiO_2 (wt.%), (b) CaO (wt.%) vs. Zr (ppm), (c) Fe_2O_3 (wt.%) vs. Al_2O_3 (wt.%), (d) K_2O (wt.%) vs. Na_2O (wt.%), (e) Rb (ppm) vs. Sr (ppm), (f) Ni (ppm) vs. Cr (ppm). For comparison, the RUF1, SO1, PDS1, and IS6 clays and the contemporaneous and attested Campanian productions are plotted. Data are from Morra et al. (2013); Grifa et al. (2013, 2015); De Bonis et al. (2013, 2016); Greco et al. (2014); Munzi et al. (2014); Guarino et al. (2016). CW, cooking ware; FW, ferruginous ware; RP, Red Pompeiian ware; TWW, thin-walled ware [Color figure can be viewed at wileyonlinelibrary.com]

Problematic for this proposition, however, is the fact that De Bonis et al.'s analysis also revealed that the specimen of Sant'Agnello clay subjected to analysis exhibited only very low plasticity due to the limited presence of clay minerals. In accord with this result is the fact that one contemporary Maiano brick and tile maker interviewed about the raw materials that he employs stated that the ceramic paste that he uses is not suitable for throwing pottery on account of its limited plasticity (Peña & Kane, 2016). This craftsman indicated that for his work, he employs what he regards as two distinct kinds of clay that he obtains in the Sant'Agnello area, terming these *creta* (clay) and *creta più terrosa* (more earthy clay), sieving both of these materials to remove pebble-size inclusions and then combining them in the proportion of 70%–80% *creta* to 30%–20% *creta più terrosa*. This suggests that there is significant, and, to some degree,

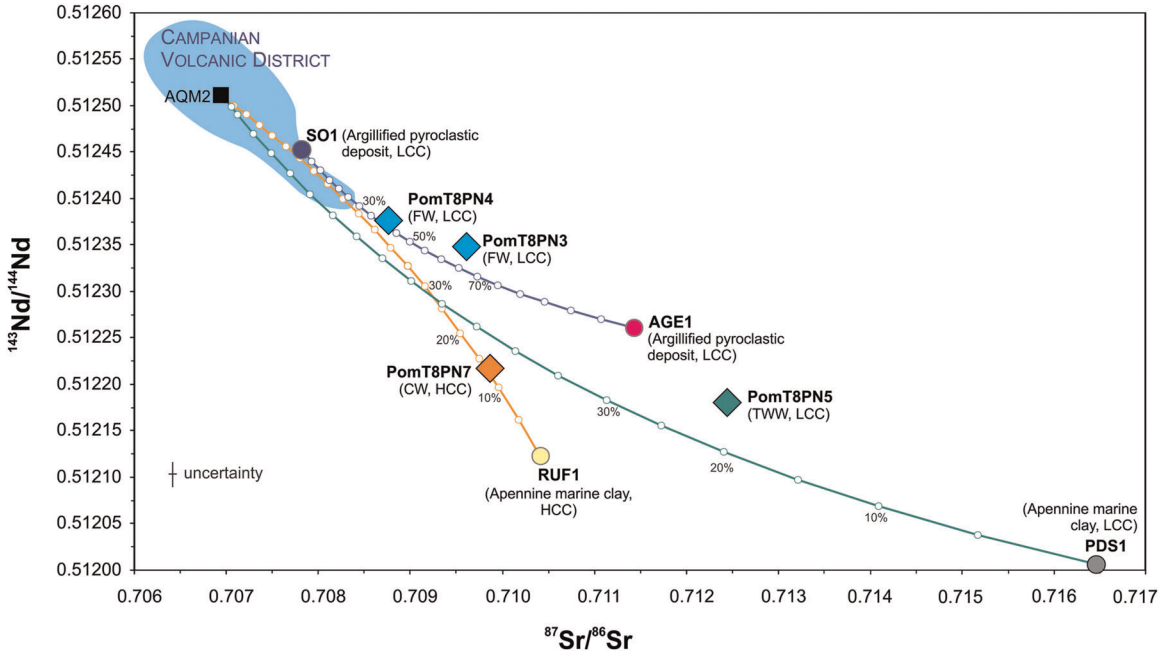

FIGURE 11 $^{87}Sr/^{86}Sr$ and $^{143}Nd/^{144}Nd$ isotope ratios of PomT8PN7 (CW), PomT8PN5 (TWW), PomT8PN3 (FW), and PomT8PN4 (FW) from Pompeii, AGE1 clay (argillified pyroclastic deposit) and RUF1 and PDS1 clays (Apennine marine clays). Two mixing curves between RUF1 (orange line) and PDS1 (green line) clays mixed with AQM2 temper and a mixing line extending from SO1 and AGE1 clays (blue line) are elaborated. The light blue field represents the isotopic composition of Neapolitan volcanic products (data from Brown et al., 2014; D'Antonio et al., 2007, 2013, 2016; Di Renzo et al., 2007, 2011). Symbols as in Figure 10. CW, cooking ware; FW, ferruginous ware; HCC, high-CaO clay; LCC, low-CaO clay; TWW, thin-walled ware [Color figure can be viewed at wileyonlinelibrary.com]

systematic variability in the texture of the clays that can be obtained at different locales within the Sant'Agnello area and/or at different depths below the current ground surface. This raises the possibility that although the material from some of these locations is unsuitable for the production of pottery due to its low plasticity, material from other places in the Sant'Agnello area might be suitable for this purpose if subjected to the requisite processing regimen.

Indeed, isotopic analysis showed affinity between the FW group and the Sorrento clay, also suggesting a mixing with another volcanic-derived clay. This would indicate that a mixing process, such as the one described above, was implemented also in the past to correct plasticity and improve processing. In fact, the composition of argillified pyroclastic deposits in the area exhibits a certain variability, and it is likely that in the area of S. Agnello, there may be a material with a composition more similar to that of AGE1. The robustness of the isotope method showed differences between the two analyzed FW specimens that indicate the proportions of the abovementioned mixture.

As far as transportation is concerned, we have to consider that the ports at Pompeii and Surrentum were separated by ca. 8.5 nautical miles (15.7 km) of open water (https://www.nauticando.net/servizi-per-la-navigazione/navigazione-waypoint/), and the two towns would have been intervisible. If we assume that in many cases, the voyage from one to the other could have been completed at an average speed of between 2 and 4 knots (3.7–7.4 km/h), we can estimate a one-way travel time of between 2.125 and 4.25 h, and there must have been regular, perhaps even intensive traffic between the two ports. It, thus, seems plausible to conjecture that there was some regular arrangement for the shipping of Piano di Sorrento clay and/or Sant'Agnello clay to Pompeii (perhaps along with several other locations around the Bay of Naples), or that potters at Pompeii arranged a boat owner to undertake a trip to the harbor at Surrentum or to some point along the coast closer to the Sant'Agnello clay source area for the purpose of acquiring a load of one or the other of these two materials, or to put in at one of these locations for this purpose in the course of a trip being made for some other purpose.

As noted above, a set of four passages in the ancient literary sources supports the inference that Surrentum was a source of clay that was extensively employed for the manufacture of pottery by craftsmen who operated in this area during more or less the same period as that when the pottery that is the subject of this program of analysis was manufactured. The most interesting of these is an epigram in the *Anthologia Graeca* (11.27), probably composed at some point between the 30s and 50s CE, which indicates that Surrentum possessed a highly regarded potting clay that it terms *trecheîa* (rough) and *myrípnoe* (sweet breathing), implying that this was employed for the manufacture of vessels for the drinking and/or the storage/packaging of wine. A passage in Pliny the Elder's *Historia Naturalis* (31.60), probably written in the years immediately before 77 CE, states that Surrentum was renowned for the production of a type of vessel termed a *calix*, which is probably to be understood as a vessel for the drinking of wine. An epigram by Martial, probably composed at the end of the first or the very beginning of the

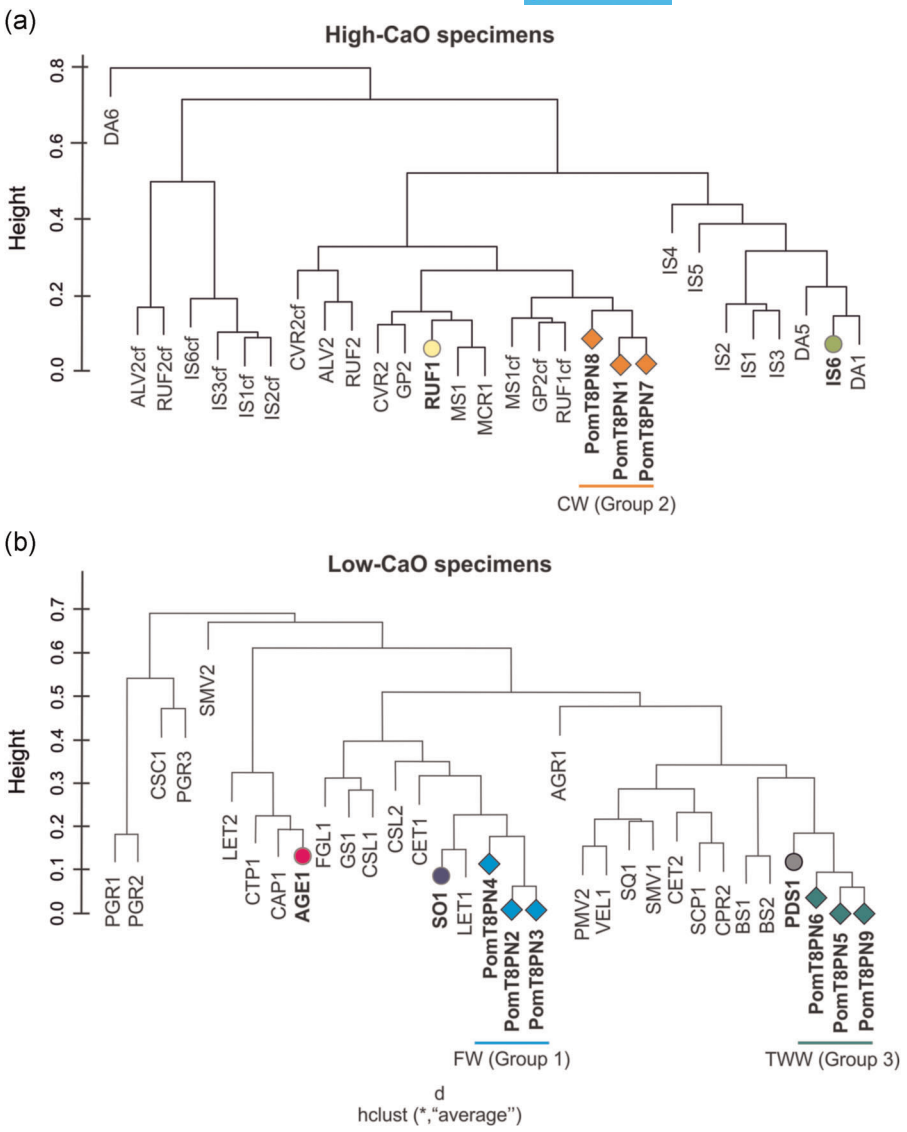

FIGURE 12 Hierarchical cluster analysis dendrogram resulting from multivariate statistical analyses of chemical data for high-CaO (a) and low-CaO (b) specimens (pottery and clays). Labels of samples ending with "cf" indicate the respective clay fraction of some selected specimens (De Bonis et al., 2013). Additional information on clay specimens is reported in Table S2. Symbols as in Figure 10 [Color figure can be viewed at wileyonlinelibrary.com]

second-century CE, refers to *calices* from Surrentum (14.102), and, finally, a second epigram by this author, composed at the same time, indicates that Surrentum manufactured vessels for both the storage/packaging of the wine that it produced (presumably amphorae) and for the drinking of this wine (presumably *calices*).

Taken together, these passages indicate that the Surrentum area possessed sources of coarse or gritty clay that was employed throughout much of the first-century CE for the manufacture of amphorae and wine-drinking vessels, or perhaps sources of two distinct clays, given the different performance properties generally required for the manufacture of these two quite different kinds of vessels. In light of this observation and the ease with which it would have been possible to transport clay from the Surrentum area to Pompeii by sea, it seems possible that the FW group, which consists principally of heavy, utilitarian forms analogous to amphorae, was manufactured in a coarser paste produced using volcanic-derived Sant-Agnello clay, whereas the TWW group, which is composed mainly of drinking vessels, was manufactured in a finer paste produced using marine Piano di Sorrento clay.

Additional important information related to firing technology was obtained by means of XRPD and SEM analyses on the nine specimens included in the program of analysis and selected for one or more readily apparent production defects that point to irregular firing. We refer to equivalent firing temperature (EFT) as mineralogical and microstructural transformations occurring upon firing, depending not only on maximum firing temperature but also on time and redox conditions of the kiln atmosphere (De Bonis et al., 2017).

For the FW specimens (Group 1), the regular presence of hematite in samples PomT8PN2 and PomT8PN4 (Table 4) points to prevailing oxidizing firing conditions and EFT not lower than 750°C (Nodari et al., 2007), whereas remainders of illite/mica indicate that the EFT would not have exceeded 950°C (De Bonis et al., 2014). The presence of hematite and hercynite in the third specimen (PomT8PN3) points to both oxidizing and reducing firing conditions, whereas mullite indicates EFT higher than 1000°C (Morra et al., 2013). This is also consistent with the continuous vitrification (Table 4 and Figure 9a) of the matrix observed in this specimen (Maniatis & Tite, 1981).

For the CW specimens (Group 2), the illite/mica in traces in one of these (PomT8PN8) indicates EFT closer to 950°C, whereas traces of analcime could be related to post-earthen weathering of pottery (Schwedt et al. 2006). The absence of illite/mica in the other two CW samples (Table 4) would suggest that firing exceeded 950°C. Moreover, the higher amounts of pyroxene detected in CW specimens contrast with the amount of the same mineral observed in the temper via OM, thus suggesting its occurrence as newly formed phases as well (e.g., Izzo et al., 2021). Newly formed pyroxene starts to form at about 850°C and increases its amount with the temperature. The continuous vitrification (Figure 9b) detected in the specimen in this group for which SEM analysis was performed (PomT8PN7) suggests a firing temperature higher than 1000°C. However, the presence of newly formed gehlenite (Table 4) allowed for a more precise estimation, indicating that EFT would not have exceeded 1050°C (De Bonis et al., 2014).

For the TWW specimens (Group 3), the presence of hematite in all three indicates prevailing oxidizing firing conditions. Traces of illite/mica in two of these (PomT8PN5 and PomT8PN6) point to EFT not higher than 950°C, whereas in the other specimen, EFT could be slightly higher (Table 4). The extensive vitrification (Figure 9c) of the matrix in the specimen for which SEM analysis was performed (PomT8PN5) suggests a maximum firing temperature, somewhat lower than that attested for the specimens belonging to the other two groups observed at SEM, most likely in the range of 850–950°C (Maniatis & Tite, 1981).

7 | CONCLUSIONS

This study involved the physical and compositional characterization of nine pottery specimens belonging to three different groups that were recovered in the excavation of a set of refuse middens deposited against the exterior of the fortification wall of Pompeii. These specimens, apparently manufactured at some point during the last quarter of the first century BCE or the first half of the first century CE, bear manufacturing defects that together with the very high firing temperatures (up to 1200°C), indicate that they are wasters presumably originating at a nearby pottery workshop. They can thus inform us about various aspects of pottery production at Pompeii.

The results indicate that one of the three groups—carbonate ware (Group 2) consisting of jars and basins with a light-colored body, was manufactured using a high-CaO clay to which volcanic sand was added as temper. The composition of the clay is compatible with that attested for marine clay from an outcrop at Rufoli di Ogliara in the outskirts of Salerno, 28 km to the east–southeast of Pompeii, and may well be from this source.

The tempering material is volcanic sand deriving from a formation belonging to the Somma-Vesuvius Volcanic Complex that was likely beach sand collected along the shore of the Bay of Naples to the north of the mouth of the Sarno River, probably at no great distance from Pompeii.

The other two wares—ferruginous ware (Group 1)—consisting of utilitarian vessels with a coarse, ferruginous body—and thin-walled ware (Group 3)—consisting of thin-walled drinking vessels in a gritty, ferruginous body—were both manufactured with a low-CaO clay and contain coarse volcanic inclusions that might be either a natural component of this clay or added temper. The nature and specific provenance of the raw materials employed to manufacture these two groups remain uncertain and need to be explored further through geological survey and compositional analysis. Most likely, both groups were manufactured with clays from the Sorrento area, on the north coast of the Sorrentine Peninsula, ca. 13–15 km to the southwest of Pompeii. The results of the program of the analysis suggest that for the ferruginous ware (Group 1) vessels manufacture likely involved the use of a mixture of clays obtained from argillified pyroclastic deposits locally available in the Sorrentine Peninsula. For the thin-walled ware (Group 3) vessels, chemical and isotopic analysis suggest that manufactured involved the use of a low-CaO marine varicolored clay such as that outcropping as olistostromes of varicolored clays in the Castelvetere wedge-top deposits on the Sorrentine Peninsula.

These results are significant for the evidence that they provide regarding the sources of the raw materials that Pompeiian potters employed to manufacture the wares that they produced, as it suggests that for a significant portion of their output these craftsmen utilized, clays from sources lying beyond the immediate environs of the town that probably reached Pompeii by sea. To the extent that pottery production at Pompeii involved the use of clays from distant sources, transported by sea via the port at Salernum and Surrentum, that was perhaps distributed to multiple production centers around the greater Bay of Naples Region and possibly even beyond, the ambiguities introduced by this practice will complicate the recognition of ceramic compositional attributes—mineralogical, chemical, and isotopic—that can be regarded as diagnostic of an origin at Pompeii.

ACKNOWLEDGMENTS

The authors would like to thank the *Parco Archeologico di Pompei* and, in particular, Prof. Massimo Osanna, Direttore Generale, and Prof. Grete Stefani, Direttrice dell'Area Archeologica di Pompei, for permission to undertake both the archaeological and archaeometric components of the research reported in this article and for collaboration and assistance in various aspects of these operations. The authors also thank Dr. Luana Toniolo for her support during the sampling. The authors would like to thank Massimo D'Antonio for his scientific advice and technical support for Sr–Nd isotopic data and Ilenia Arienzo for her help in the Sr–Nd isotopic data curation. The authors also wish to thank Aldo Cinque for providing a clay sample from Agerola. J. Theodore Peña would like to thank the members of the PALHIP field team for the 2014–2106 seasons—Aaron Brown, Laure Marest-Caffey, Caroline Cheung, and Gina Tibbott—for their contributions to the evaluation and documentation of the materials from Tower 8/Porta di Nola middens. Valuable guidance in the evaluation of the thin-walled wares from these features was

generously provided by Illuminata Faga. J. Theodore Peña would also like to acknowledge the financial support for the archaeological research provided by the University of California, Berkeley Archaeological Research Facility Stahl Fund and the University of California, Berkeley Department of Classics Klio Professorship and Heller Fund. The authors would like to acknowledge the constructive comments of two anonymous reviewers and the advice of Kevin Walsh and Sarah Sherwood, co-editors of *Geoarchaeology—An International Journal*, which were very useful for the preparation of a revised manuscript, and the scientific editing by Ian Moffat. This study was supported by grants from the Dipartimento di Scienze della Terra, dell' Ambiente e delle Risorse (Vincenzo Morra) of the Università degli Studi di Napoli Federico II.

DATA AVAILABILITY STATEMENT

The data that supports the findings of this study are available in the tables and Supporting Information materials of this article.

ORCID

Vincenza Guarino http://orcid.org/0000-0003-4313-5493
Alberto De Bonis http://orcid.org/0000-0002-8088-9481

REFERENCES

Albore Livadie, C., Barra, D., Bonaduce, G., Brancaccio, L., Cinque, A., Ortolani, F., Pagliuca, S., & Russo, F. (1990). Evoluzione geomorfologica, neotettonica e vulcanica della piana costiera del fiume Sarno (Campania) in relazione agli insediamenti anteriori all'eruzione del 79 d.C. *Pact*, *25*, 237–256.

Arnold, D. (2006). The threshold model for ceramic resources: A refinement. In D. Gheorghiu (Ed.), *Ceramic studies: Papers on social and cultural significance of ceramics in Europe and Eurasia from prehistoric to historic times* (Vol. 1553, pp. 3–9). British Archaeological Reports International Series.

Avanzinelli, R., Lustrino, M., Mattei, M., Melluso, L., & Conticelli, S. (2009). Potassic and ultrapotassic magmatism in the circum-Tyrrhenian region: Significance of carbonated pelitic vs. pelitic sediment recycling at destructive plate margins. *Lithos*, *113*(1–2), 213–227.

Babazadeh, S., D'Antonio, M., Cottle, J. M., Ghalamghash, J., Raeisi, D., & An, Y. (2021). Constraints from geochemistry, zircon U-Pb geochronology and Hf-Nd isotopic compositions on the origin of Cenozoic volcanic rocks from central Urumieh-Dokhtar magmatic arc, Iran. *Gondwana Research*, *90*, 27–46.

Barra, D., Cinque, A., Italiano, A., & Scorziello, R. (1992). Il Pleistocene superiore marino di Ischia: paleoecologia e rapporti con l'evoluzione tettonica recente. *Studi Geologici Camerti*, *Special Issue*, *1*, 231–243.

Brown, R. J., Civetta, L., Arienzo, I., D'Antonio, M., Moretti, R., Orsi, G., Tomlinson, E. L., Albert, P. G., & Menzies, M. A. (2014). Geochemical and isotopic insights into the assembly, evolution and disruption of a magmatic plumbing system before and after a cataclysmic caldera-collapse eruption at Ischia volcano (Italy). *Contributions to Mineralogy and Petrology*, *168*, 1–23. https://doi.org/10.1007/s00410-014-1035-1

Buchner, G. (1994). I giacimenti di argilla dell'isola d'Ischia e l'industria figulina locale in età recente, In G. Donatone (Ed.), *Centro studi per la storia della ceramica meridionale*, (pp. 17–45). Uniongrafica Corcelli.

Casson, L. (1951). Speed under sail of ancient ships. *Transactions of the American Philological Association*, *82*, 136–148.

Cavassa, L. (2009). La production de céramique commune à Pompéi. Un four de potier dans L'insula 5 de la regio I. In M. Pasqualini (Ed.), Les céramiques communes d'Italie et de Narbonnaise. Structures de production, typologies et contexts inédits IIe s. av. J.-C.–*IIIe s. apr. J.-C. Actes de la table ronde de Naples organisée les 2 et 3 novembre 2006* (pp. 95–104). Collection du Centre Jean Bérard 30.

Cavassa, L., Lacombe, A., & Lemaire, B. (2015). Une production de gobelets à paroi fine à Pompéi en 79 de notre ère, Société française d'étude de la céramique antique en Gaule. *Actes du congrès de Nyon*, *14–17 mai 2015* (pp. 285–292).

Cavassa, L., Lemaire, B., & Piffeteau, J. M. (2013). Pompéi. L'atelier de potier Via dei Sepolcri, boutique NE, n. 29, In *Chronique des activités archéologiques de l'École française de Rome 2013, DOI : 10.4000/cefr. 881*. https://cefr.revues.org/881

Cesarano, M., Bish, D., Cappelletti, P., Cavalcante, F., Belviso, C., & Fiore, S. (2018). Quantitative mineralogy of clay-rich siliciclastic landslide terrain of the Sorrento Peninsula, Italy, using a combined XRPD and XRF approach. *Clays and Clay Minerals*, *66*, 353–369. https://doi.org/10.1346/CCMN.2018.064108

Chiaramonte Trerè, C. (Ed.). (1986). *Nuovi contributi sulle fortificazioni pompeiane*. Quaderni di Acme.

Cinque, A. (1991). La trasgressione versiliana nella Piana del Sarno (Campania). *Geografia Fisica e Dinamica Quaternaria*, *14*, 63–71.

Cinque, M. (2015). The archaeological potential of Agerola (Amalfi Coast, S. Italy) in relation to geological factors. *Proceedings of the 1st International Conference on Metrology for Archaeology, Benevento (Italy)*, October 22–23, 2015, pp. 135–139, ISBN: 978-88-940453-3-8.

Conticelli, S., Melluso, L., Perini, G., Avanzinelli, R., & Boari, E. (2004). Petrologic, geochemical and isotopic characteristics of shoshonitic to potassic and ultrapotassic alkalic magmatism in central-southern Italy: Inferences on its genesis and on the nature of its mantle source. *Periodico di Mineralogia*, *73*, 135–164.

Cucciniello, C., Le Roex, A. P., Jourdan, F., Morra, V., Grifa, C., Franciosi, L., & Melluso, L. (2018). The mafic alkaline volcanism of SW Madagascar (Ankililoaka, Tulear region): $^{40}Ar/^{39}Ar$ ages, geochemistry and tectonic setting. *Journal of the Geological Society*, *175*, 627–641. https://doi.org/10.1144/jgs2017-139

Cucciniello, C., Melluso, L., Le Roex, A. P., Jourdan, F., Morra, V., de' Gennaro, R., & Grifa, C.(2017). From olivine nephelinite, basanite and basalt to peralkaline trachyphonolite and comendite in the Ankaratra volcanic complex, Madagascar: $^{40}Ar/^{39}Ar$ ages, phase compositions and bulk-rock geochemical and isotopic evolution. *Lithos*, 274–275, 363–382.

D'Antonio, M., Mariconte, R., Arienzo, I., Mazzeo, F. C., Carandente, A., Perugini, D., Petrelli, M., Corselli, C., Orsi, G., Principato, M. S., & Civetta, L. (2016). Combined Sr-Nd isotopic and geochemical fingerprinting as a tool for identifying tephra layers: Application to deep-sea cores from Eastern Mediterranean Sea. *Chemical Geology*, *443*, 121–136. https://doi.org/10.1016/j.chemgeo.2016.09.022

D'Antonio, M., Tonarini, S., Arienzo, I., Civetta, L., Dallai, L., Moretti, R., Orsi, G., Andria, M., & Trecalli, A. (2013). Mantle and crustal processes in the magmatism of the Campania region: Inferences from mineralogy, geochemistry, and Sr-Nd-O isotopes of young hybrid volcanics of the Ischia island (South Italy). *Contributions to Mineralogy and Petrology*, *165*, 1173–1194. https://doi.org/10.1007/s00410-013-0853-x

D'Antonio, M., Tonarini, S., Arienzo, I., Civetta, L., & Di Renzo, V. (2007). Components and processes in the magma genesis of the Phlegrean Volcanic District, southern Italy. In L. Beccaluva, G. Bianchini, & M. Wilson (Eds.), Cenozoic volcanism in the Mediterranean area. Geological Society of America Special Papers (Vol. 418, pp. 203–220). https://doi.org/10.1130/2007.2418(10)

De Bonis, A., Arienzo, I., D'Antonio, M., Franciosi, L., Germinario, C., Grifa C., Guarino V., Langella A., & Morra V. (2018). Sr-Nd isotopic fingerprinting as a tool for ceramic provenance: Its application on raw materials, ceramic replicas and ancient pottery. *Journal of Archaeological Science*, *94*, 51–59. https://doi.org/10.1016/j.jas.2018.04.002

De Bonis, A., Cultrone, G., Grifa, C., Langella, A., & Morra, V. (2014). Clays from the Bay of Naples (Italy): New insight on ancient and traditional ceramics. *Journal of the European Ceramic Society*, *34*, 3229–3244. https://doi.org/10.1016/j.jeurceramsoc.2014.04.014

De Bonis, A., D'Angelo, M., Guarino, V., Massa, S., Anaraki, F. S., Genito, B., & Morra, V. (2017). Unglazed pottery from the masjed-i jom'e of Isfahan (Iran): Technology and provenance. *Archaeological and Anthropological Sciences*, *9*, 617–635. https://doi.org/10.1007/s12520-016-0407-z

De Bonis, A., Febbraro, S., Germinario, C., Giampaola, D., Grifa, C., Guarino, V., Langella, A., & Morra, V. (2016). Distinctive volcanic material for the production of Campana A Ware: The workshop area of Neapolis at the Duomo Metro Station in Naples, Italy. *Geoarchaeology*, *31*, 437–466. https://doi.org/10.1002/gea.21571

De Bonis, A., Grifa, C., Cultrone, G., De Vita, P., Langella, A., & Morra, V. (2013). Raw materials for archaeological pottery from the Campania region of Italy: A petrophysical characterization. *Geoarchaeology*, *28*, 478–503. https://doi.org/10.1002/gea.21450

Di Renzo, V., Arienzo, I., Civetta, L., D'Antonio, M., Tonarini, S., Di Vito, M. A., & Orsi, G. (2011). The magmatic feeding system of the Campi Flegrei caldera: Architecture and temporal evolution. *Chemical Geology*, *281*, 227–241.

Di Renzo, V., Di Vito, M. A., Arienzo, I., Civetta, L., D'Antonio, M., Giordano, F., Orsi, G., & Tonarini, S. (2007). Magmatic history of Somma-Vesuvius on the basis of new geochemical and isotopic data from a deep borehole (Camaldoli della Torre). *Journal of Petrology*, *48*, 753–784.

Ellis, S. J. R., Emmerson, A. L. C., Dicus, K., Tibbott, G., & Pavlick, A. K. (2015). The 2012 field season at I.10.1-10, Pompeii: Preliminary report on the excavations. *Fasti Online Documents & Research*, 328. http://www.fastionline.org/docs/FOLDER-it-2015-328.pdf

Fabbri, B., Guarini, G., Arduino, E., & Coghé, M. (1994). Significato del fosforo nei reperti ceramici di scavo. In F. Burragato, O. Grubbessi, & L. Lazzarini (Eds.), *Proceedings of the 1st European workshop on archaeological ceramics*, Roma, 10–12 ottobre 1991, pp. 183–192.

Franciosi, L., D'Antonio, M., Fedele, L., Guarino, V., Tassinari, C. C. G., de' Gennaro, R., & Cucciniello, C. (2019). Petrogenesis of the Solanas gabbro-granodiorite intrusion, Sàrrabus (southeastern Sardinia, Italy): Implications for Late Variscan magmatism. *International Journal of Earth Sciences*, *108*(3), 989–1012. https://doi.org/10.1007/s00531-019-01689-8

Garzanti, E., Canclini, S., Moretti Foggia, F., Petrella, N. (2002). Unraveling magmatic and orogenic provenance in modern sand: The back-arc side of the Apennine thrust belt, Italy. *Journal of Sedimentary Research*, *72*, 2–17. https://doi.org/10.1306/051801720002

Greco, G., Tomeo, A., Ferrara, B., Guarino, V., De Bonis, A., & Morra, V. (2014). Cumae, the forum: Typological and archaeometric analysis of some pottery classes from sondages inside the temple with portico. In G. Greco & L. Cicala (Eds.), *Archaeometry: Comparing experiences* (Vol. 19, pp. 37–68). Quaderni del Centro Studi Magna Grecia.

Greene, K. (1986). *The archaeology of the Roman economy*. University of California Press.

Grifa, C., Cavassa, L., De Bonis, A., Germinario, C., Guarino, V., Izzo, F., Kakoulli, I., Langella, A., Mercurio, M., & Morra, V. (2016). Beyond vitruvius: New insight in the technology of Egyptian blue and green frits. *Journal of the American Ceramic Society*, *99*(10), 3467–3475. https://doi.org/10.1111/jace.14370

Grifa, C., De Bonis, A., Guarino, V., Petrone, C. M., Germinario, C., Mercurio, M., Soricelli, G., Langella, A., & Morra, V. (2015). Thin walled pottery from Alife (Northern Campania, Italy). *Periodico di Mineralogia*, *84*, 65–90. https://doi.org/10.2451/2015PM0005

Grifa, C., De Bonis, A., Langella, A., Mercurio, M., Soricelli, G., & Morra, V. (2013). A Late Roman ceramic production from Pompeii. *Journal of Archaeological Science*, *40*(2), 810–826.

Grifa, C., Germinario, C., De Bonis, A., Cavassa, L., Izzo, F., Mercurio, M., Langella, A., Kakoulli, I., Fischer, C., Barra, D., Aiello, G., Soricelli, G., Vyhnal, C. R., & Morra, V. (2021a). A pottery workshop in Pompeii unveils new insights on the Roman ceramics crafting tradition and raw materials trade. *Journal of Archaeological Science*, *126*, 105305. https://doi.org/10.1016/j.jas.2020.105305

Grifa, C., Germinario, C., De Bonis, A., Cavassa, L., Izzo, F., Mercurio, M., Langella, A., Kakoulli, I., Fischer, C., Barra, D., Aiello, G., Soricelli, G., Vyhnal, C. R., & Morra, V. (2021b). Archaeometric data from the Via dei Sepolcri ceramic workshop in Pompeii (Southern Italy). *Data in Brief*, *34*, 106706. https://doi.org/10.1016/j.dib.2020.106706

Grifa, C., Germinario, C., De Bonis, A., Langella, A., Mercurio, M., Izzo, F., Smiljanic, D., Guarino, V., Di Mauro, S., & Soricelli, G. (2019). Comparing ceramic technologies: The production of *Terra Sigillata* in *Puteoli* and in the Bay of Naples. *Journal of Archaeological Science: Reports*, *23*, 291–303. https://doi.org/10.1016/j.jasrep.2018.10.014.

Grifa, C., Morra, V., Langella, A., & Munzi, P. (2009). Byzantine ceramic production from Cuma (Campi Flegrei, Napoli). *Archaeometry*, *51*, 75–94. https://doi.org/10.1111/j.1475-4754.2008.00416.x

Guarino, V., De Bonis, A., Faga, I., Giampaola, D., Grifa, C., Langella, A., Liuzza, V., Pierobon Benoit, R., Romano, P., & Morra, V. (2016). Production and circulation of thin walled pottery from the Roman port of Neapolis, Campania (Italy). *Periodico di Mineralogia*, *85*(1), 95–114. https://doi.org/10.2451/2016PM618

Guarino, V., de' Gennaro, R., Melluso, L., Ruberti, E., & Azzone, R.G. (2019). The transition from miaskitic to agpaitic rocks as marked by the accessory mineral assemblages, in the Passa Quatro alkaline complex (southeastern Brazil). *Canadian Mineralogist*, *57*, 339–361. https://doi.org/10.3749/canmin.1800073

Hall, M. E. (2004). Pottery production during the Late Jomon period: Insights from the chemical analyses of Kasori B pottery. *Journal of Archaeological Science*, *31*, 1439–1450.

Istituto Superiore per la Protezione e la Ricerca Ambientale (ISPRA). Carta geologica d'Italia alla scala 1:50.000, Campania, Foglio 466–485 Sorrento-Termini.

Izzo, F., Guarino, V., Ciotola, A., Verde, M., De Bonis, A., Capaldi, C., & Morra, V. (2021). An archaeometric investigation in a consumption context: Exotic, imitation and traditional ceramic productions from the Forum of Cumae (southern Italy). *Journal of Archaeological Science: Reports*, *35*, 102768. https://doi.org/10.1016/j.jasrep.2020.102768

Joron, J. L., Metrich, N., Rosi, M., Santacroce, R., & Sbrana, A. (1987). Chemistry and petrography. In R. Santacroce (Ed.), *Somma-Vesuvius* (Vol. 8, pp. 105–174). CNR Quaderni della Ricerca Scientifica.

Kelly, S. E., Watkins, C. N., & Abbott, D. R. (2011). Revisiting the exploitable threshold model: 14th century resource procurement and landscape dynamics on Perry Mesa, Arizona. *Journal of Field Archaeology*, *36*, 322–336.

Kibaroğlu, M., Kozal, E., Klügel, A., Hartmann, G., & Monien, P. (2019). New evidence on the provenance of Red Lustrous Wheel-made Ware (RLW): Petrographic, elemental and Sr-Nd isotope analysis. *Journal of Archaeological Science: Reports*, *24*, 412–433. https://doi.org/10.1016/j.jasrep.2019.02.004

Langmuir, C. H., Vocke Jr., R. D., & Hanson, G. H. (1978). A general mixing equation with applications to Icelandic basalts. *Earth and Planetary Science Letters*, *37*(1), 380–392.

Locock, A. J. (2008). An Excel spreadsheet to recast analyses of garnet into end-member components, and a synopsis of the crystal chemistry of natural silicate garnets. *Computers & Geosciences*, *34*, 1769–1780.

Maggetti, M. (2001). Chemical analyses of ancient ceramics: What for? *Chimia*, *55*, 923–930.

Maniatis, Y., & Tite, M. S. (1981). Technological examination of Neolithic-Bronze Age pottery from central and southeast Europe and from the Near East. *Journal of Archaeological Science*, *8*, 59–76.

Mannoni, T. (1984). Caratterizzazioni mineralogico-petrografiche di alcune classi di reperti. In M. Bonghi Jovino (Ed.), *Ricerche a Pompei: L'insula 5 della Regio VI dalle origini al 79 d.C.* (Vol. 1, pp. 346–351). Campagne di scavo.

Melluso, L., de' Gennaro, R., Fedele, L., Franciosi, L. & Morra, V. (2012). Evidence of crystallization in residual, Cl-F-rich, agpaitic, trachyphonolitic magmas and primitive Mg-rich basalt-trachyphonolite interaction in the lava domes of the Phlegrean Fields (Italy). *Geological Magazine*, *149*, 532–550.

Melluso, L., Morra, V., Guarino, V., de' Gennaro, R., Franciosi, L., & Grifa, C. (2014). The crystallization of shoshonitic to peralkaline trachyphonolitic magmas in a H_2O-Cl-F-rich environment at Ischia (Italy), with implications for the feeder system of the Campania Plain volcanoes. *Lithos*, *210–211*, 242–259. http://dx.doi.org/10.1016/j.lithos.2014.10.002

Morimoto, N. (1988). Nomenclature of pyroxenes. *American Mineralogist*, *73*, 1123–1133.

Morra, V., Aiello, G., Amore, O., Arienzo, I., Barra, D., Cavassa, L., D'Antonio, M., De Bonis, A., Germinario, C., Grifa, C., Guarino, V., Langella, A., & Mercurio, M. (2020). Indagini archeometriche di carattere minero-petrografico su ceramiche da Pompei. In L. Toniolo, & M. Osanna (Eds.), *Fecisti Cretaria. Produzione e circolazione ceramica a Pompei. Stato degli studi e prospettive di ricerca* (pp. 33–39).

Morra, V., Calcaterra, D., Cappelletti, P., Colella, A., Fedele, L., de' Gennaro, R., Langella, A., Mercurio, M., & de' Gennaro, M. (2010). Urban geology: Relationships between geological setting and architectural heritage of the Neapolitan area. In M. Beltrando, A. Peccerillo, M. Mattei, S. Conticelli, & C. Doglioni (Eds.), *The geology of Italy: Tectonics and life along plate margins. Journal of the Virtual Explorer*, *36*, paper 27. https://doi.org/10.3809/jvirtex.2010.00261

Morra, V., De Bonis, A., Grifa, C., Langella, A., Cavassa, L., & Piovesan, R. (2013). Minero-petrographic study of cooking ware and Pompeian red ware (Rosso Pompeiano) from Cuma (Southern Italy). *Archaeometry*, *55*(5), 852–879. https://doi.org/10.1111/j.1475-4754.2012.00710.x

Munzi, P., Guarino, V., De Bonis, A., Morra, V., Grifa, C., & Langella, A. (2014). Fourth century black-glaze ware from the Northern Periurban Sanctuary of Cumae. In G. Greco, & L. Cicala (Eds.), *Archaeometry: Comparing experiences* (Vol. 19, pp. 69–87). Quaderni del Centro Studi Magna Grecia.

Nodari, L., Marcuz, E., Maritan, L., Mazzoli, C., & Russo, U. (2007). Hematite nucleation and growth in the firing of carbonate-rich clay for pottery production. *Journal of the European Ceramic Society*, *27*, 4665–4673. https://doi.org/10.1016/j.jeurceramsoc.2007.03.031

Olcese, G. (2011). *Le anfore greco italiche di Ischia: archeologia ed archeometria*. Immensa Aequora (p. 480). Edizioni Quasar.

Orton, C., & Hughes, M. (Eds.). (2013). Pottery in archaeology & *Cambridge manuals in archaeology* (2nd ed.). Cambridge University Press. https://doi.org/10.1017/CBO9780511920066

Peña, J. T. (1992). Raw material use among nucleated industry potters: The case of Vasanello, Italy, *Archeomaterials*, *6*(2), 93–122.

Peña, J. T. (2020). Evidence for pottery production from the Torre VIII/Porta di Nola refuse middens at Pompeii. In L. Toniolo & M. Osanna (Eds.), *Fecisti Cretaria. Produzione e circolazione ceramica a Pompei. Stato degli studi e prospettive di ricerca* (pp. 23–32).

Peña, J. T., & Kane, H. (2016). La creta fatta concreta: project narrative. *RES ROMANAE*. University of California, Berkeley Roman Material Culture Laboratory. http://resromanae.berkeley.edu/node/3701

Peña, J. T., & McCallum, M. (2009a). The production and distribution of pottery at Pompeii: A review of the evidence; Part 2, the material basis for production and distribution. *American Journal of Archaeology*, *113*(2), 165–201. https://doi.org/10.3764/aja.113.2.165

Peña, J. T., & McCallum, M. (2009b). The production and distribution of pottery at Pompeii: A review of the evidence; Part 1, production. *American Journal of Archaeology*, *113*(1), 57–79. https://doi.org/10.3764/aja.113.1.57

Pouchou, J. L., & Pichoir, F., 1988. A simplified version of the 'PAP' model for matrix corrections in EPMA. In D. Newbury (Ed.), *Microbeam Analysis* (p. 315).

Pryor, J. H. (1989). The voyage of Rutilius Namatianus: From Rome to Gaul in 417 CE. *Mediterranean Historical Review*, *4*, 271–280. https://doi.org/10.1080/09518968908569573

Renson, V., Jacobs, A., Coenaerts, J., Mattielli, N., Nys, K., & Claeys, P. (2013). Using lead isotopes to determine pottery provenance in Cyprus: Clay source signatures and comparison with Late Bronze Age Cypriote pottery. *Geoarchaeology*, *28*(6), 517–530. https://doi.org/10.1002/gea.21454

Renson, V., Martínez-Cortizas, A., Mattielli, N., Coenaerts, J., Sauvage, C., De Vleeschouwer, F., Lorre, C., Vanhaecke, F., Bindler, R., Rautman, M., Nys, K., & Claeys, P. (2013). Lead isotopic analysis within a multi-proxi approach to trace pottery sources. The example of White Slip II sherds from Late Bronze Age sites in Cyprus and Syria. *Applied Geochemistry*, *28*, 220–234.

Renson, V., Slane, K. W., Rautman, M. L., Kidd, B., Guthrie, J., & Glascock, M. D. (2016). Pottery provenance in the Eastern Mediterranean using lead isotopes. *Archaeometry*, *58*, 54–67. https://doi.org/10.1111/arcm.12217

Rispoli, C., De Bonis, A., Guarino, V., Graziano, S. F., Di Benedetto, C., Esposito, R., Morra, V., & Cappelletti, P. (2019). The ancient pozzolanic mortars of the thermal complex of Baia (Campi Flegrei, Italy). *Journal of Cultural Heritage*, *40*, 143–154. https://doi.org/10.1016/j.culher.2019.05.010

Romanazzi, L., & Volontè, A. M. (1986). Gli scarichi tra Porta Nola e la Torre. In C. Chiaramonte Trerè (Ed.), *Nuovi contributi sulle fortificazioni pompeiane* (Vol. 6, pp. 55–113). Quaderni di Acme.

Scarpelli, R., Clark, R. J. H., & De Francesco, A. M. (2014). Archaeometric study of black-coated pottery from Pompeii by different analytical techniques. *Spectrochimica Acta Part A: Molecular and Biomolecular Spectroscopy*, *120*, 60–66.

Scarpelli, R., Robustelli, G., Clark Robin, J. H., & De Francesco, A. M. (2017). Scientific investigations on the provenance of the black glazed pottery from Pompeii: A case study. *Mediterranean Archaeology and Archaeometry*, *17*(2), 1–10.

Scheibner, B., Wörner, G., Civetta, L., Stosch, H. G., Simon, K., & Kronz, A. (2007). Rare earth element fractionation in magmatic Ca-rich garnets. *Contributions to Mineralogy and Petrology*, *154*, 55–74.

Schwedt, A., Mommsen, H., Zacharias, N., & Buxeda I Garrigós, J. (2006). Analcime crystallization and compositional profiles—Comparing approaches to detect post-depositional alterations in archaeological pottery. *Archaeometry*, *48*(2), 237–251.

Seiler, F., Märker, M., Kastenmeier, P., Vogel, S., Esposito, D., Heussner, U., Boni, M., Balassone, G., Di Maio, G., & Joachimski, M. (2011). Interdisciplinary approach on the reconstruction of the ancient cultural landscape of the Sarno River Plain before the eruption of Somma-Vesuvius A. D. 79. *Tagungen des Landesmuseums für Vorgeschichte Hall*, *6*, 1–10.

Terry R. D., & Chilingar, G. V. (1955). Summary of concerning some additional aids in studying sedimentary formations. *Journal of Sedimentary Petrology*, *25*, 229–234.

Toniolo, L., & Osanna, M. (Eds.). (2020). *Fecisti Cretaria. Produzione e circolazione ceramica a Pompei. Stato degli studi e prospettive di ricerca.*

Vitale, S., & Ciarcia, S. (2018). Tectono-stratigraphic setting of the Campania region (southern Italy). *Journal of Maps*, *14*(2), 9–21. https://doi.org/10.1080/17445647.2018.1424655

Vogel, S., Märker, M., & Seiler, F. (2011). Revised modelling of the post-AD 79 volcanic deposits of Somma-Vesuvius to reconstruct the pre-AD 79 topography of the Sarno River plain (Italy).

Geologica Carpathica, *62*, 5–16. https://doi.org/10.2478/v10096-011-0001

Whitney, D. L., & Evans, B. W. (2010). Abbreviations for names of rock-forming minerals. *American Mineralogist*, *95*, 185–187.

SUPPORTING INFORMATION

Additional Supporting Information may be found online in the supporting information tab for this article.

How to cite this article: Guarino, V., De Bonis, A., Peña, J. T., Verde, M., & Morra, V. (2021). Multianalytical investigation of wasters from the Tower 8/Porta di Nola refuse middens in Pompeii: Sr–Nd isotopic, chemical, petrographic, and mineralogical analyses. *Geoarchaeology*, 1–28. https://doi.org/10.1002/gea.21858